An inverse problem for a semilinear parabolic equation arising from cardiac electrophysiology

Elena Beretta[1], **Cecilia Cavaterra**[2], **M Cristina Cerutti**[1], **Andrea Manzoni**[3] and **Luca Ratti**[1]

[1] Dipartimento di Matematica, Politecnico di Milano, P.za Leonardo da Vinci 32, I-20133 Milano, Italy

[2] Dipartimento di Matematica, Università degli Studi di Milano, via Saldini 50, I-20133 Milano, Italy

[3] CMCS-MATH-SB, Ecole Polytechnique Fédérale de Lausanne, Station 8, CH-1015 Lausanne, Switzerland

E-mail: elena.beretta@polimi.it, cristina.cerutti@polimi.it, luca.ratti@polimi.it, cecilia.cavaterra@unimi.it and andrea.manzoni@epfl.ch

Received 5 April 2017, revised 18 July 2017
Accepted for publication 21 August 2017
Published 20 September 2017

Abstract

In this paper we develop theoretical analysis and numerical reconstruction techniques for the solution of an inverse boundary value problem dealing with the nonlinear, time-dependent monodomain equation, which models the evolution of the electric potential in the myocardial tissue. The goal is the detection of an inhomogeneity ω_ϵ (where the coefficients of the equation are altered) located inside a domain Ω starting from observations of the potential on the boundary $\partial\Omega$. Such a problem is related to the detection of myocardial ischemic regions, characterized by severely reduced blood perfusion and consequent lack of electric conductivity. In the first part of the paper we provide an asymptotic formula for electric potential perturbations caused by internal conductivity inhomogeneities of low volume fraction in the case of three-dimensional, parabolic problems. In the second part we implement a reconstruction procedure based on the topological gradient of a suitable cost functional. Numerical results obtained on an idealized three-dimensional left ventricle geometry for different measurement settings assess the feasibility and robustness of the algorithm.

Keywords: inverse boundary value problem, semilinear parabolic equation, cardiac electrophysiology

1. Introduction

The rigorous mathematical analysis of inverse boundary value problems involving nonlinear evolution equations presents many intrinsic difficulties. On the other hand, several contributions have shown the effectiveness of numerical procedures adopted to tackle problems within this class. In this context, we provide here a combined framework, addressing an inverse problem arising in cardiac electrophysiology from both the theoretical viewpoint and the computational perspective.

This paper deals with an inverse problem of potential interest in cardiac electrophysiology, namely the detection of the position of myocardial ischemias from measurements of the electric potential. From a mathematical standpoint, this turns into the problem of locating small inhomogeneities inside a domain, where the coefficients of the equation are altered, starting from observations of the solution of the equation on the boundary.

1.1. Motivations

Mathematical and numerical models of computational electrophysiology can provide quantitative tools to describe electrical heart function and disfunction [42], often complementing imaging techniques (such as computed tomography and magnetic resonance) for diagnostic and therapeutic purposes. In this context, detecting pathological conditions or reconstructing model features such as tissue conductivities from potential measurements yield to the solution of an inverse boundary value problem. Standard electrocardiographic techniques attempt to infer electrophysiological processes in the heart from body surface measurements of the electrical potential, as in the case of electrocardiograms (ECGs), or body surface ECGs (also known as body potential maps). These measurements can provide useful insights for the reconstruction of the cardiac electrical activity within the so-called electrocardiographic imaging, by solving the well-known inverse problem of electrocardiography[4]. A much more invasive option to acquire potential measurements is represented by non-contact electrodes inside a heart cavity to record endocardial potentials.

Here we focus on the problem of detecting the position and the size of myocardial ischemias from a single boundary measurement of the electric potential. Ischemia is a reversible precursor of heart infarction caused by partial occlusion of one or more coronary arteries, which supply blood to the heart. If this condition persists, myocardial cells die and the ischemia eventually degenerates in infarction. For the time being, we consider an insulated heart model, neglecting the coupling with the torso; this results in the inverse problem of detecting inhomogeneities for a nonlinear parabolic reaction-diffusion equation (in our case, the so-called monodomain equation) dealing with a single measurement of the endocardial potential. Our long-term goal is indeed to deal with an inverse problem for the coupled heart-torso model, in order to detect ischemias from body surface measurements, such as those acquired on each patient with symptoms of cardiac disease through an ECG.

1.2. Mathematical background and novelties

An extensively studied class of inverse problems for parabolic equations includes, for instance, the determination of diffusion coefficients as well as of reaction terms (even partially) and, to

[4] The *inverse problem of electrocardiography* aims at recovering the epicardial potential (that is, at the heart surface) from body surface measurements [20, 21, 41]. Since the torso is considered as a passive conductor, such an inverse problem involves the linear steady diffusion model as direct problem. A step further, aiming at computing the potential inside the heart from the epicardial potential, has been considered, e.g. in [14].

a lesser extent, also the identification of unknown inclusions in the spatial domain (see, e.g. [30, 8, 31, 36] and references therein). Several techniques have been proposed to obtain different kinds of results. However, in this general framework, the main difficulties consist in the choice (and number) of additional data and in the fact that even in the linear cases the corresponding inverse problems turn out to be nonlinear.

The problem we consider in this paper is a mathematical challenge itself, never considered before from a rigorous analytical viewpoint. Indeed, here the difficulties include the nonlinearity of both the direct and the inverse problem, as well as the lack of measurements at disposal. We underline that even for the linear counterpart of the inverse problem, it has been shown in [24] and [32] that infinitely many measurements are needed to detect uniquely the unknown inclusions, and that the continuous dependence of the inclusion from the data is logarithmic [22].

Moreover, despite the fact that inverse problem of ischemia identification from measurements of surface potentials has been tackled in an optimization framework for numer-ical purposes [1, 18, 29, 35, 37], a detailed mathematical analysis of this problem has never been performed, mainly due to the presence of nonlinearities. To our knowledge, no rigor-ous theoretical invest igation of inverse problems related with ischemia detection involving the monodomain and/or the bidomain model has been carried out. On the other hand, recent results regarding both the analysis and the numerical approximation of this inverse problem in a much simpler stationary case have been obtained in [9, 10]. Additional assumptions are needed to obtain rigorous theor etical results, for instance by considering small-size conductiv-ity inhomogeneities. We thus model ischemic regions as small inclusions ω_ϵ where the electric conductivity is significantly smaller than the one of healthy tissue and there is no ion transport.

We establish a rigorous asymptotic expansion of the boundary potential perturbation due to the presence of the inclusion adapting to the parabolic nonlinear case the approach introduced by Capdeboscq and Vogelius in [15] for the case of the linear conductivity equation. The theory of detection of small conductivity inhomogeneities from boundary measurements via asymptotic techniques has been developed in the last three decades in the framework of Electric Impedence Tomography (see, e.g. [5, 16, 26]). A similar approach has also been used in Thermal Imaging (see, e.g. [4]). We use these results to set a reconstruction procedure for detecting the inclusion. To this aim, as in [10], we propose a reconstruction algorithm based on topological optimization, where a suitable quadratic functional is minimized to detect the position of the inclusion under a small size assumption (see also [17]). This requires the solution of two initial and boundary value problems, the background problem and the adjoint one, which are discretized by means of a Galerkin finite element method. Numerical results obtained on an idealized left ventricle geometry assess the feasibility of the proposed procedure. Several numerical test cases also show the robustness of the reconstruction procedure with respect to measurement noise, unavoidable when dealing with real data. The modeling assumption on the small size of the inclusion, instrumental to the derivation of our theoretical results, is verifed in practice in the case of residual ischemias after myocardial infarction. On the other hand, a fundamental task of ECG's imaging is to detect the presence of ischemias as precursor of heart infarction without any constraint on its size. For this reason, we also consider the case of the detection of larger size inclusions, for which the proposed algorithm still provides useful insights.

The paper is organized as follows. In section 2 we describe the monodomain model of cardiac electrophysiology we are going to consider. In section 3 we show some suitable well posedness results concerning the direct problems, in the unperturbed (background) and perturbed cases. In section 4 we prove useful energy estimates of the difference of the solutions of the two previous problems. The asymptotic expansion formula is derived in section 5 and

the reconstruction algorithm in section 6. Numerical results are finally provided in section 7. The appendix, section 8, is devoted to technical proofs of some results in sections 5 and 6.

2. The monodomain model of cardiac electrophysiology

The monodomain equation is a nonlinear parabolic reaction-diffusion PDE for the transmembrane potential, describing the macroscopic electric activity of the heart [20, 47]. Throughout the paper we consider the following (background) initial and boundary value problem

$$\begin{cases} \nu C_m u_t - \operatorname{div}(k_0 \nabla u) + \nu f(u) = 0, & \text{in } \Omega \times (0,T), \\ \frac{\partial u}{\partial n} = 0, & \text{on } \partial\Omega \times (0,T), \\ u(0) = u_0, & \text{in } \Omega, \end{cases} \tag{1}$$

where $\Omega \subset \mathbf{R}^3$ is a bounded set with boundary $\partial\Omega$, and $k_0 \in \mathbb{R}, k_0 > 0$. Here Ω is the domain occupied by the ventricle, u is the (transmembrane) electric potential, $f(u)$ is a nonlinear term modeling the ionic current flows across the membrane of cardiac cells, k_0 is the conductivity tensor of the healthy tissue, $C_m > 0$ and $\nu > 0$ are two constant coefficients representing the membrane capacitance and the surface area-to-volume ratio, respectively. In our case, the model (1) is indeed widely used to characterize the large-scale propagation of the front-like solution in the cardiac excitable medium. For the sake of simplicity we deal with an insulated heart, namely we do not consider the effect of the surrounding torso, which behaves as a passive conductor. The initial datum u_0 represents the initial activation of the tissue, arising from the propagation of the electrical impulse in the cardiac conduction system. This equation yields a macroscopic model of the cardiac tissue, arising from the superposition of intra and extra cellular media, both assumed to occupy the whole heart volume (bidomain model), making the hypothesis that the extracellular and the intracellular conductivities are proportional quantities. Concerning the mathematical analysis of both the monodomain and the bidomain models, some results on the related direct problems have been obtained for instance in [7, 11, 13, 20].

We thus assume a phenomenological model to describe the effect of ionic currents through a nonlinear function of the potential. We neglect the coupling with the ODE system modeling the evolution of the so-called *gating variables*, which represent the amount of open channels per unit area of the cellular membrane and thus regulate the transmembrane currents.

In the case of a single gating variable w, a well-known option would be to replace f by

$$g(u,w) = -\beta u(u-\alpha)(u-1) - w,$$

and w solves the following ODE initial value problem, $\forall\, x \in \Omega$,

$$\frac{\partial w}{\partial t} = \rho(u - \gamma w) \ \text{ in } (0,T), \qquad w(0) = w_0,$$

for suitable (constant) parameters β, α, ρ, γ. This is the so-called FitzHugh–Nagumo model for the ionic current, and the gating variable w is indeed a recovery function describing the refractariness of cells and thus accounting for the depolarization phase. More sophisticated ventricular cell models feature several gating variables and more complex nonlinearities in the ionic current expression; see, e.g. [20, 42, 47] for an in-depth overview.

As suggested in [20, section 4.2] and [47, section 2.2], hereon we consider the cubic function

$$f(u) = A^2(u-u_1)(u-u_2)(u-u_3), \quad u_i \in \mathbb{R}, \quad u_1 < u_2 < u_3, \tag{2}$$

where $A > 0$ is a parameter determining the rate of change of u in the depolarization phase, and $u_1 < u_2 < u_3$ are given constant values representing the resting, threshold and peak potentials, respectively. Possible values of the parameters are, e.g. $u_1 = -85$ mV, $u_2 = -65$ mV and $u_3 = 40$ mV, $A = 0.04$, see [47]. Note that both the sharpness of the wavefront and its propagation speed strongly depend on the value of the parameter A.

Consider now a small inhomogeneity located in a measurable bounded domain $\omega_\varepsilon \subset \Omega$, such that there exist a compact set K_0, with $\omega_\varepsilon \subset K_0 \subset \Omega$, and a constant $d_0 > 0$ satisfying

$$\operatorname{dist}(\omega_\varepsilon, \Omega \backslash K_0) \geqslant d_0 > 0. \tag{3}$$

Moreover, we assume

$$|\omega_\varepsilon| > 0, \qquad \lim_{\varepsilon \to 0} |\omega_\varepsilon| = 0. \tag{4}$$

In the inhomogeneity ω_ε the conductivity coefficient and the nonlinearity take different values with respect the ones in $\Omega \backslash \omega_\varepsilon$. The problem we consider is therefore

$$\begin{cases} \nu C_m u_t^\varepsilon - \operatorname{div}(k_\varepsilon \nabla u^\varepsilon) + \nu \chi_{\Omega \backslash \omega_\varepsilon} f(u^\varepsilon) = 0, & \text{in } \Omega \times (0,T), \\ \frac{\partial u^\varepsilon}{\partial n} = 0, & \text{on } \partial\Omega \times (0,T), \\ u^\varepsilon(0) = u_0, & \text{in } \Omega, \end{cases} \tag{5}$$

where χ_D stands for the characteristic function of a set $D \subset \mathbb{R}^3$. Here

$$k_\varepsilon = (k_0 - k_1)\chi_{\Omega \backslash \omega_\varepsilon} + k_1 = \begin{cases} k_0 & \text{in } \Omega \backslash \omega_\varepsilon, \\ k_1 & \text{in } \omega_\varepsilon, \end{cases} \tag{6}$$

with $k_0, k_1 \in \mathbb{R}$, $k_0 > k_1 > 0$.

Indeed, according to biological observations, cells in an infarcted area are no longer excitable, and the electrical conductivity in this portion of tissue is much smaller than the one of healthy tissue. As a matter of fact, we incorporate the presence of an ischemia into the model (5) by diverting (forcing) the ion transport to go around the infarcted areas, and by varying the conductivity in such regions, similarly to what proposed in [35].

Remark 2.1. In order to embed information about prior knowledge on the shape of the ischemia, several different parametrizations of the conductivity fields can be considered. For instance, in [35, 45] the parameters of a level set function are used to describe a non-homogeneous conductivity tensor and the related ionic current. A different approach is taken into account in [1, 18], where the presence of an ischemia is instead described in terms of two (non-homogeneous in space) parameters of the ionic model; see also, e.g. [12] for similar considerations. In this paper we rather focus on the identification of ischemias which can be assimilated to circles, whose position and dimension are unknown; note that the whole setting can be extended also to non connected ischemias—recent experimental measurements indeed show that ischemic regions are neither monolithic nor simply localized, see, e.g. [6]—described by a finite number of (small) well-separated inhomogeneities.

3. Well posedness of the direct problem

Problem (1) thus describes the propagation of the initial activation u_0 in an insulated heart portion (e.g. the left ventricle), and hereon will be referred to as the *background problem*; we devote section 3.1 to the analysis of its well-posedness. The well-posedness of the perturbed problem modeling the presence of a small inclusion in the domain will be instead analyzed in section 3.2.

3.1. Well posedness of the background problem

For the sake of simplicity, throughout the paper we set $\nu = C_m = 1$ and we assume that

$$\Omega \in C^{2+\alpha},\ \alpha \in (0,1), \tag{7}$$

$$u_0 \in C^{2+\alpha}(\overline{\Omega}), \qquad u_1 < u_0(x) < u_3 \quad \forall\, x \in \Omega, \qquad \frac{\partial u_0(\sigma)}{\partial n} = 0 \quad \forall\, \sigma \in \partial\Omega. \tag{8}$$

Moreover, let us set

$$M_1 := \|f\|_{C([u_1,u_3])}, \qquad M_2 := \|f'\|_{C([u_1,u_3])}. \tag{9}$$

The following well posedness result holds.

Theorem 3.1. *Let us assume (2), (7) and (8). Then problem (1) admits a unique solution* $u \in C^{2+\alpha,1+\alpha/2}(\overline{\Omega} \times [0,T])$ *such that*

$$u_1 \leqslant u(x,t) \leqslant u_3, \quad (x,t) \in \overline{\Omega} \times [0,T], \tag{10}$$

$$\|u\|_{C^{2+\alpha,1+\alpha/2}(\overline{\Omega}\times[0,T])} \leqslant C, \tag{11}$$

where C is a positive constant depending (at most) on $k_0, T, \Omega, M_1, M_2, \|u_0\|_{C^{2+\alpha}(\overline{\Omega})}$. **Proof.** We omit the details of the proof since (10) can be easily obtained using the results in [39, definition 3.1 and theorem 4.1] and (11) by means of [34, theorem 5.1.17 (ii) and theorem 5.1.20].

3.2. Well posedness of the perturbed problem

Hereon, for the sake of brevity, we will omit in all the integrals the dependence on the space variable and/or on the time variable of the integrated functions, unless it is necessary to avoid misunderstandings. Moreover, all inequalities depending on t are valid for $t \in (0,T)$.

The well-posedness of the perturbed problem (5) is provided by the following theorem.

Theorem 3.2. *Assume (2) and (6)–(8). Then problem (5) admits a unique weak solution* u^ε *such that*

$$u^\varepsilon \in L^2(0,T;H^1(\Omega)) \cap C([0,T];L^2(\Omega)), \quad u^\varepsilon_t \in L^2(0,T;(H^1(\Omega))') + L^{4/3}(\Omega \times (0,T)). \tag{12}$$

Moreover, $u^\varepsilon \in C^{\alpha,\alpha/2}(\overline{\Omega} \times [0,T])$ *and the following estimate holds*

$$\|u^\varepsilon\|_{C^{\alpha,\alpha/2}(\overline{\Omega}\times[0,T])} \leqslant C, \tag{13}$$

where C is a positive constant depending (at most) on $k_0, k_1, T, \Omega, \|u_0\|_{C^\alpha(\overline{\Omega})}$ *and* M_1.

Proof. Throughout the proof C will be as in the statement of the Theorem. Recalling the definition of f, there exist $k \geqslant 0$, $\alpha_1 > 0$, $\alpha_2 > 0$, $\lambda > 0$ such that

$$\alpha_1 u^4 - k \leqslant f(u)u \leqslant \alpha_2 u^4 + k, \qquad f'(u) \geqslant -\lambda.$$

We formulate problem (5) in the weak form

$$\int_\Omega u_t^\varepsilon v\mathrm{d}x + \int_\Omega k_\varepsilon \nabla u^\varepsilon \cdot \nabla v\mathrm{d}x + \int_\Omega \chi_{\Omega\setminus\omega_\varepsilon} f(u^\varepsilon) v\mathrm{d}x = 0,\ \forall v \in H^1(\Omega). \tag{14}$$

Setting $\tilde{f}(u) = f(u) - u$, (14) becomes

$$\int_\Omega u_t^\varepsilon v\mathrm{d}x + \int_\Omega k_\varepsilon \nabla u^\varepsilon \cdot \nabla v\mathrm{d}x + \int_\Omega \chi_{\Omega\setminus\omega_\varepsilon} u^\varepsilon v\mathrm{d}x + \int_\Omega \chi_{\Omega\setminus\omega_\varepsilon} \widetilde{f}(u^\varepsilon) v\mathrm{d}x = 0, \quad \forall v \in H^1(\Omega). \tag{15}$$

Observe that, thanks to following the Poincaré type inequality in [9, formula (A.4)]

$$\|z\|^2_{H^1(\Omega)} \leqslant S(\Omega)\left(\|\nabla z\|^2_{L^2(\Omega)} + \|z\|^2_{L^2(\Omega\setminus\omega_\varepsilon)}\right), \quad \forall z \in H^1(\Omega), \tag{16}$$

the bilinear form $a_\varepsilon(u^\varepsilon, v) = \left(\int_\Omega k_\varepsilon \nabla u^\varepsilon \cdot \nabla v\mathrm{d}x + \int_{\Omega\setminus\omega_\varepsilon} u^\varepsilon v\right)$ is coercive. Indeed

$$a_\varepsilon(u^\varepsilon, u^\varepsilon) = \int_\Omega k_\varepsilon |\nabla u^\varepsilon|^2 \mathrm{d}x + \int_{\Omega\setminus\omega_\varepsilon} (u^\varepsilon)^2 \mathrm{d}x \geqslant S\|u^\varepsilon\|^2_{H^1(\Omega)}, \tag{17}$$

where S is a positive constant depending on Ω and k_1. Through the classical Faedo–Galerkin approximation scheme it is possible to prove that problem (5) admits a unique weak solution u^ε satisfying (12). In order to obtain further regularity for u^ε, let $\{\phi_n\}$ be a sequence such that

$$\phi_n \in C^1(\overline{\Omega}),\ 0 \leqslant \phi_n(x) \leqslant 1,\ \forall x \in \overline{\Omega},\ \phi_n(x) = 1,\ \forall x \in \overline{\Omega}\setminus\omega_\varepsilon,\ \text{and } \phi_n \to \chi_{\Omega\setminus\omega_\varepsilon} \text{ in } L^\infty(\Omega),$$

and formulate the approximating problems

$$\begin{cases} u_t^n - \mathrm{div}(((k_0 - k_1)\phi_n + k_1)\nabla u^n) + \phi_n f(u^n) = 0, & \text{in } \Omega \times (0,T), \\ \frac{\partial u^n}{\partial n} = 0, & \text{on } \partial\Omega \times (0,T), \\ u^n(0) = u_0, & \text{in } \Omega. \end{cases} \tag{18}$$

Using the same arguments as in the proof of theorem 3.1, we can prove that, $\forall n \in \mathbb{N}$, problem (18) admits a unique solution u^n such that

$$u^n \in C(\overline{\Omega} \times [0,T]), \quad u_1 \leqslant u^n(x,t) \leqslant u_3, \quad (x,t) \in \overline{\Omega} \times [0,T].$$

Moreover, by means again of a standard Faedo–Galerkin approximation scheme (for any n) we can prove that the solution to problem (18) satisfies also

$$u^n \in L^2(0,T;H^1(\Omega)), \quad u_t^n \in L^2(0,T;(H^1(\Omega))') + L^{4/3}(\Omega \times (0,T)),$$

$$\|u^n\|^2_{L^2(0,T;H^1(\Omega))} \leqslant C, \qquad \|u_t^n\|^2_{L^{4/3}(0,T;(H^1(\Omega))')} \leqslant C, \qquad \|\phi_n \widetilde{f}(u^n)\|^2_{L^{4/3}(\Omega\times(0,T))} \leqslant C,$$

where C are some positive constants independent of n.

An application of [43, theorem 8.1] implies that, up to a subsequence, $u^n \to \zeta$ strongly in $L^2(\Omega \times (0,T))$, so that $u^n \to \zeta$ a.e. in $\Omega \times (0,T)$ and $\phi_n \widetilde{f}(u^n) \rightharpoonup \chi_{\omega_\varepsilon} \widetilde{f}(\zeta)$ in $L^{4/3}(\Omega \times (0,T))$. Since problem (5) has a unique solution (see (14)), we conclude that $\zeta = u^\varepsilon$ and satisfies

$$\|u^\varepsilon\|^2_{L^2(0,T;H^1(\Omega))} \leqslant C, \quad \|u_t^\varepsilon\|^2_{L^{4/3}(0,T;(H^1(\Omega))')} \leqslant C, \quad u_1 \leqslant u^\varepsilon(x,t) \leqslant u_3, \quad \text{in } \overline{\Omega} \times [0,T]. \tag{19}$$

Considering now the interior regularity result in [23, theorem 2.1] (see also [33]) and the regularity up to the boundary contained in [23, theorem 4.1], then we deduce (13).

4. Energy estimates for $u^\varepsilon - u$

In this section we prove some energy estimates for the difference between u^ε and u, solutions to problem (5) and problem (1), respectively, that are crucial to establish the asymptotic formula for $u^\varepsilon - u$ of theorem 5.1 in section 3.

Proposition 4.1. *Assume (2) and (6)–(8). Setting $w := u^\varepsilon - u$, then*

$$\|w\|_{L^\infty(0,T;L^2(\Omega))} \leqslant C|\omega_\varepsilon|^{1/2}, \tag{20}$$

$$\|w\|_{L^2(0,T;H^1(\Omega))} \leqslant C|\omega_\varepsilon|^{1/2}. \tag{21}$$

Moreover, there exists $0 < \beta < 1$ such that

$$\|w\|_{L^2(\Omega\times(0,T))} \leqslant C|\omega_\varepsilon|^{\frac{1}{2}+\beta}. \tag{22}$$

Here C stands for a positive constant depending (at most) on $k_0, k_1, \Omega, T, M_1, M_2, \|u_0\|_{C^{2+\alpha}(\overline{\Omega})}$.

Proof. Throughout the proof C will be as in the statement of the theorem. According to the hypotheses, theorems 3.1 and 3.2 hold. Then w solves the problem

$$\begin{cases} w_t - \operatorname{div}(k_\varepsilon \nabla w) + \chi_{\Omega/\omega_\varepsilon} p_\varepsilon w = -\operatorname{div}(\widetilde{k}\chi_{\omega_\varepsilon}\nabla u) + \chi_{\omega_\varepsilon} f(u), & \text{in } \Omega\times(0,T), \\ \frac{\partial w}{\partial n} = 0, & \text{on } \partial\Omega\times(0,T), \\ w(0) = 0, & \text{in } \Omega, \end{cases} \tag{23}$$

where we have set $\widetilde{k} := k_0 - k_1 > 0$ and

$$p_\varepsilon w := f'(z_\varepsilon)w = f(u^\varepsilon) - f(u), \tag{24}$$

z_ε satisfying $u^\varepsilon(x,t) \leqslant z_\varepsilon(x,t) \leqslant u(x,t)$. By means of (10), (19) and recalling (9), we have

$$u_1 \leqslant z_\varepsilon \leqslant u_3, \qquad |p_\varepsilon| = |f'(z_\varepsilon)| \leqslant M_2, \quad \text{in } \overline{\Omega}\times[0,T]. \tag{25}$$

Multiplying the first equation by w in (23) by w and integrating by parts over Ω, we get

$$\frac{1}{2}\frac{\mathrm{d}}{\mathrm{d}t}\int_\Omega w^2\mathrm{d}x + \int_\Omega k_\varepsilon|\nabla w|^2\mathrm{d}x + \int_\Omega \chi_{\Omega/\omega_\varepsilon} p_\varepsilon w^2\mathrm{d}x = \int_\Omega \widetilde{k}\chi_{\omega_\varepsilon}\nabla u\cdot\nabla w\mathrm{d}x + \int_\Omega \chi_{\omega_\varepsilon} f(u)w\mathrm{d}x.$$

Adding and subtracting $\int_\Omega \chi_{\Omega\setminus\omega_\varepsilon}(x)w^2(x)\mathrm{d}x$ and applying (17) we obtain

$$\frac{1}{2}\frac{\mathrm{d}}{\mathrm{d}t}\int_\Omega w^2\mathrm{d}x + S\|w\|^2_{H^1(\Omega)} \leqslant \int_{\omega_\varepsilon}\widetilde{k}\nabla u\cdot\nabla w\mathrm{d}x + \int_{\omega_\varepsilon} f(u)w\mathrm{d}x - \int_\Omega \chi_{\Omega/\omega_\varepsilon}(p_\varepsilon - 1)w^2\mathrm{d}x.$$

Recalling (9) and (25), thanks to Young's inequality we deduce

$$\frac{1}{2}\frac{\mathrm{d}}{\mathrm{d}t}\int_\Omega w^2\mathrm{d}x + S\|w\|^2_{H^1(\Omega)}$$
$$\leqslant \widetilde{k}\left(\frac{\widetilde{k}}{2S}\int_{\omega_\varepsilon}|\nabla u|^2\mathrm{d}x + \frac{S}{2\widetilde{k}}\int_\Omega |\nabla w|^2\mathrm{d}x\right) + \frac{1}{2}\int_{\omega_\varepsilon}(f(u))^2\mathrm{d}x + \int_\Omega\left(M_2+\frac{3}{2}\right)w^2\mathrm{d}x,$$

so that

$$\frac{1}{2}\frac{\mathrm{d}}{\mathrm{d}t}\int_\Omega w^2\mathrm{d}x + \frac{S}{2}\|w\|^2_{H^1(\Omega)} \leqslant \frac{(\widetilde{k})^2}{2S}\int_{\omega_\varepsilon}|\nabla u|^2\mathrm{d}x + \frac{1}{2}\int_{\omega_\varepsilon}M_1^2\mathrm{d}x + \left(M_2+\frac{3}{2}\right)\int_\Omega w^2\mathrm{d}x, \tag{26}$$

and finally, see (11),

$$\frac{\mathrm{d}}{\mathrm{d}t}\|w(t)\|^2_{L^2(\Omega)} \leqslant C\left(|\omega_\varepsilon| + \|w(t)\|^2_{L^2(\Omega)}\right).$$

Recalling that $w(0)=0$, an application of Gronwall's lemma implies

$$\|w(t)\|^2_{L^2(\Omega)} \leqslant C|\omega_\varepsilon|, \quad t\in(0,T), \tag{27}$$

and (20) follows. Integrating now inequality (26) on $(0,T)$ we get

$$\int_\Omega w^2(T)\mathrm{d}x + C\int_0^T \|w(t)\|^2_{H^1(\Omega)}\mathrm{d}t \leqslant C\left(|\omega_\varepsilon| + \int_0^T \|w(t)\|^2_{L^2(\Omega)}\mathrm{d}t\right),$$

and a combination with (27) gives (21).

In order to obtain the more refined estimate (22), observe that w also solves problem

$$\begin{cases} w_t - \mathrm{div}(k_0\nabla w) + \chi_{\Omega/\omega_\varepsilon}p_\varepsilon w = -\mathrm{div}(\widetilde{k}\chi_{\omega_\varepsilon}\nabla u^\varepsilon) + \chi_{\omega_\varepsilon}f(u), & \text{in } \Omega\times(0,T),\\ \frac{\partial w}{\partial n} = 0, & \text{on } \partial\Omega\times(0,T),\\ w(0)=0, & \text{in } \Omega. \end{cases} \tag{28}$$

Let us now introduce the auxiliary function $\overline{w}$, solution to the adjoint problem

$$\begin{cases} \overline{w}_t + \mathrm{div}(k_0\nabla\overline{w}) - \chi_{\Omega/\omega_\varepsilon}p_\varepsilon\overline{w} = -w, & \text{in } \Omega\times(0,T),\\ \frac{\partial\overline{w}}{\partial n} = 0, & \text{on } \partial\Omega\times(0,T),\\ \overline{w}(T)=0, & \text{in } \Omega. \end{cases} \tag{29}$$

By the change of variable $t\to T-t$, problem (29) is equivalent to

$$\begin{cases} \underline{z_t} - \mathrm{div}(k_0\nabla z) + \chi_{\Omega/\omega_\varepsilon}\hat{p}_\varepsilon z = \hat{w}, & \text{in } \Omega\times(0,T),\\ \frac{\partial z}{\partial n} = 0, & \text{on } \partial\Omega\times(0,T),\\ z(0)=0, & \text{in } \Omega, \end{cases} \tag{30}$$

where we have set $z(x,t)=\overline{w}(x,T-t)$, $\hat{p}_\varepsilon(x,t)=p_\varepsilon(x,T-t)$, $\hat{w}(x,t)=w(x,T-t)$.

Since $|\chi_{\Omega/\omega_\varepsilon}\hat{p}_\varepsilon|$ is bounded in $\overline{\Omega}\times[0,T]$ and $w\in C^{\alpha,\alpha/2}(\overline{\Omega}\times[0,T])$, standard arguments show that problem (30) admits a unique solution z such that (see [33, section 4])

$$z \in W_2^{2,1}(\Omega \times (0,T)) := \left\{ z \in L^2(\Omega \times (0,T)) \,|\, z \in H^1(0,T;L^2(\Omega)) \cap L^2(0,T;H^2(\Omega)) \right\}.$$

Moreover, multiplying the first equation in (30) by z and integrating over Ω, we get

$$\frac{1}{2}\frac{\mathrm{d}}{\mathrm{d}t}\int_\Omega z^2 \mathrm{d}x + k_0 \int_\Omega |\nabla z|^2 \mathrm{d}x + k_0 \int_\Omega z^2 \mathrm{d}x = \int_\Omega \hat{w} z \mathrm{d}x - \int_\Omega \chi_{\Omega/\omega_\varepsilon} \hat{p}_\varepsilon z^2 \mathrm{d}x + k_0 \int_\Omega z^2 \mathrm{d}x.$$

By means of Young's inequality and recalling (25), we have

$$\frac{1}{2}\frac{\mathrm{d}}{\mathrm{d}t}\|z(t)\|^2_{L^2(\Omega)} + \frac{k_0}{2}\|z(t)\|^2_{H^1(\Omega)} \leqslant \frac{1}{2k_0}\|\hat{w}(t)\|^2_{L^2(\Omega)} + (M_2 + k_0)\|z(t)\|^2_{L^2(\Omega)},$$

and then

$$\frac{\mathrm{d}}{\mathrm{d}t}\|z(t)\|^2_{L^2(\Omega)} \leqslant \frac{1}{k_0}\|\hat{w}(t)\|^2_{L^2(\Omega)} + 2(M_2 + k_0)\|z(t)\|^2_{L^2(\Omega)}.$$

Recalling that $z(x,0) = 0$, an application of Gronwall's lemma gives

$$\|z(t)\|^2_{L^2(\Omega)} \leqslant C\|\hat{w}(t)\|^2_{L^2(\Omega)}. \tag{31}$$

Let us now multiply the first equation in (30) by z_t and integrate over Ω. We get

$$\int_\Omega z_t^2 \mathrm{d}x + \frac{k_0}{2}\frac{\mathrm{d}}{\mathrm{d}t}\int_\Omega |\nabla z|^2 \mathrm{d}x = \int_\Omega \hat{w} z_t \mathrm{d}x - \int_\Omega \chi_{\Omega/\omega_\varepsilon} \hat{p}_\varepsilon z z_t \mathrm{d}x.$$

An application of Young's inequality gives

$$\frac{1}{2}\int_\Omega z_t^2 \mathrm{d}x + \frac{k_0}{2}\frac{\mathrm{d}}{\mathrm{d}t}\int_\Omega |\nabla z|^2 \mathrm{d}x \leqslant \int_\Omega (\hat{w})^2 \mathrm{d}x + \int_\Omega \chi_{\Omega/\omega_\varepsilon} (\hat{p}_\varepsilon)^2 z^2 \mathrm{d}x,$$

and then

$$\frac{1}{2}\|z_t(t)\|^2_{L^2(\Omega)} + \frac{k_0}{2}\frac{\mathrm{d}}{\mathrm{d}t}\|\nabla z(t)\|^2_{L^2(\Omega)} \leqslant \|\hat{w}(t)\|^2_{L^2(\Omega)} + M_2^2\|z(t)\|^2_{L^2(\Omega)}. \tag{32}$$

Combining (32) and (31), integrating in time on $(0,t)$, and using $\nabla z(0) = 0$ we deduce

$$\|\nabla z(t)\|^2_{L^2(\Omega)} \leqslant C\|\hat{w}\|^2_{L^2(\Omega\times(0,t))}, \quad t \in (0,T),$$

so that

$$\|z\|^2_{L^\infty(0,T;H^1(\Omega))} \leqslant C\|\hat{w}\|^2_{L^2(\Omega\times(0,T))}. \tag{33}$$

The same computations also give

$$\|z_t\|^2_{L^2(\Omega\times(0,T))} \leqslant C\|\hat{w}\|^2_{L^2(\Omega\times(0,T))}.$$

Then, an application of standard elliptic regularity results to problem (30) implies (see [28])

$$\|z\|^2_{L^2(0,T;H^2(\Omega))} \leqslant C\|\hat{w}\|^2_{L^2(\Omega\times(0,T))}. \tag{34}$$

Recalling the definition of z and $\hat{w}$, by estimates (33) and (34) we get

$$\|\overline{w}\|^2_{L^\infty(0,T;H^1(\Omega))} + \|\overline{w}\|^2_{L^2(0,T;H^2(\Omega))} \leqslant C\|w\|^2_{L^2(\Omega\times(0,T))}, \tag{35}$$

Finally, we want to prove that there exists $p > 2$ such that

$$\|\overline{w}\|_{L^p(\Omega\times(0,T))} + \|\nabla\overline{w}\|_{L^p(\Omega\times(0,T))} \leqslant C\|w\|_{L^2(\Omega\times(0,T))}. \tag{36}$$

To this aim, on account of (35) and Sobolev immersion theorems, we deduce

$$\|\overline{w}\|^2_{L^6(\Omega\times(0,T))} \leqslant C\|\overline{w}\|^2_{L^\infty(0,T;H^1(\Omega))} \leqslant C\|w\|^2_{L^2(\Omega\times(0,T))}.$$

Moreover, again from (35) we have

$$\nabla\overline{w} \in L^\infty(0,T;L^2(\Omega)) \cap L^2(0,T;L^6(\Omega)).$$

From well-known interpolation estimates (see [38]) we infer

$$\|\nabla\overline{w}\|^{10/3}_{L^{10/3}(\Omega\times(0,T))} \leqslant C\|\nabla\overline{w}\|^2_{L^2(0,T;L^6(\Omega))}\|\nabla\overline{w}\|^{4/3}_{L^{4/3}(0,T;L^2(\Omega))}$$

and therefore, using (35),

$$\|\nabla\overline{w}\|^{10/3}_{L^{10/3}(\Omega\times(0,T))} \leqslant C\|w\|^2_{L^2(\Omega\times(0,T))}\|w\|^{4/3}_{L^2(\Omega\times(0,T))} \leqslant C\|w\|^{10/3}_{L^2(\Omega\times(0,T))},$$

so that (36) holds for any $p \in (2, \frac{10}{3}]$.

Let us now multiply the evolution equation in (28) by $\overline{w}$ and the evolution equation in (29) by w, respectively. Integrating on Ω we obtain

$$\int_\Omega w_t\overline{w}\mathrm{d}x + k_0\int_\Omega \nabla w\cdot\nabla\overline{w}\mathrm{d}x + \int_\Omega \chi_{\Omega/\omega_\varepsilon}p_\varepsilon w\overline{w}\mathrm{d}x = \widetilde{k}\int_{\omega_\varepsilon}\nabla u^\varepsilon\cdot\nabla\overline{w}\mathrm{d}x + \int_{\omega_\varepsilon} f(u)\overline{w}\mathrm{d}x, \tag{37}$$

$$\int_\Omega \overline{w}_t w\mathrm{d}x - k_0\int_\Omega \nabla\overline{w}\cdot\nabla w\mathrm{d}x - \int_\Omega \chi_{\Omega/\omega_\varepsilon}p_\varepsilon\overline{w}w\mathrm{d}x = -\int_\Omega w^2\mathrm{d}x. \tag{38}$$

Summing up (37) and (38) we get

$$\int_\Omega (w_t\overline{w} + \overline{w}_t w)\mathrm{d}x = \widetilde{k}\int_{\omega_\varepsilon}\nabla u^\varepsilon\cdot\nabla\overline{w}\mathrm{d}x + \int_{\omega_\varepsilon} f(u)\overline{w}\mathrm{d}x - \int_\Omega w^2\mathrm{d}x,$$

subsequently, an integration in time on $(0,T)$ gives

$$\int_0^T\int_\Omega w^2\mathrm{d}x\mathrm{d}t = -\int_0^T\int_\Omega (w_t\overline{w} + \overline{w}_t w)\mathrm{d}x\mathrm{d}t + \widetilde{k}\int_0^T\int_{\omega_\varepsilon}\nabla u^\varepsilon\cdot\nabla\overline{w}\mathrm{d}x\mathrm{d}t + \int_0^T\int_{\omega_\varepsilon} f(u)\overline{w}\mathrm{d}x\mathrm{d}t. \tag{39}$$

Recalling the conditions at time $t = 0$ for w and at time $t = T$ for $\overline{w}$, we get

$$\int_\Omega \mathrm{d}x\int_0^T (w_t\overline{w} + \overline{w}_t w)\,\mathrm{d}t = \int_\Omega \Big((w\overline{w})(T) - (w\overline{w})(0) - \int_0^T (w\overline{w}_t + \overline{w}_t w)\mathrm{d}t\Big)\mathrm{d}x = 0.$$

So that (39) becomes

$$\int_0^T \int_\Omega w^2 \mathrm{d}x\mathrm{d}t = \widetilde{k} \int_0^T \int_{\omega_\varepsilon} \nabla u^\varepsilon \cdot \nabla \overline{w} \mathrm{d}x\mathrm{d}t + \int_0^T \int_{\omega_\varepsilon} f(u)\overline{w} \mathrm{d}x\mathrm{d}t. \tag{40}$$

Using now Hölder inequality we deduce

$$\|w\|^2_{L^2(\Omega\times(0,T))} \leqslant \|\nabla u^\varepsilon\|_{L^q(\omega_\varepsilon\times(0,T))} \|\nabla \overline{w}\|_{L^p(\omega_\varepsilon\times(0,T))} + \|f(u)\|_{L^q(\omega_\varepsilon\times(0,T))} \|\overline{w}\|_{L^p(\omega_\varepsilon\times(0,T))},$$

where p and q are conjugate indexes and therefore $q \in [10/7, 2)$.

By means of (36) and (9), from the previous inequality we get

$$\|w\|^2_{L^2(\Omega\times(0,T))} \leqslant C\|w\|_{L^2(\Omega\times(0,T))} \left(\|\nabla u^\varepsilon\|_{L^q(\omega_\varepsilon\times(0,T))} + |\omega_\varepsilon|^{\frac{1}{q}} \right),$$

and therefore

$$\|w\|_{L^2(\Omega\times(0,T))} \leqslant C \left(\|\nabla u^\varepsilon\|_{L^q(\omega_\varepsilon\times(0,T))} + |\omega_\varepsilon|^{\frac{1}{q}} \right). \tag{41}$$

Thanks to (11) we also have

$$\begin{aligned} \|\nabla u^\varepsilon\|_{L^q(\omega_\varepsilon\times(0,T))} &\leqslant \|\nabla u^\varepsilon - \nabla u\|_{L^q(\omega_\varepsilon\times(0,T))} + \|\nabla u\|_{L^q(\omega_\varepsilon\times(0,T))} \\ &\leqslant \|\nabla w\|_{L^q(\omega_\varepsilon\times(0,T))} + C|\omega_\varepsilon|^{\frac{1}{q}}. \end{aligned}$$

Finally, using again Hölder inequality and (21), we obtain

$$\begin{aligned} \|\nabla w\|_{L^q(\omega_\varepsilon\times(0,T))} &\leqslant \left(\int_0^T \left(\int_{\omega_\varepsilon} |\nabla w|^{q\frac{2}{q}} \mathrm{d}x \right)^{\frac{q}{2}} \left(\int_{\omega_\varepsilon} 1 \mathrm{d}x \right)^{\frac{2-q}{2}} \mathrm{d}t \right)^{\frac{1}{q}} \\ &\leqslant |\omega_\varepsilon|^{\frac{1}{q}-\frac{1}{2}} \left(\int_0^T \|\nabla w\|^2_{L^2(\Omega)} \mathrm{d}t \right)^{\frac{1}{q}} \leqslant |\omega_\varepsilon|^{\frac{1}{q}-\frac{1}{2}} \|\nabla w\|_{L^q(0,T;L^2\Omega)} \\ &\leqslant C(\Omega)|\omega_\varepsilon|^{\frac{1}{q}-\frac{1}{2}} \|\nabla w\|_{L^2(\Omega\times(0,T))} \leqslant C|\omega_\varepsilon|^{\frac{1}{q}}. \end{aligned}$$

Combining the previous estimate with (41), since $\frac{1}{q} \in (\frac{1}{2}, \frac{7}{10}]$ we can conclude that (22) holds with $\beta \in (0, \frac{1}{5}]$. □

5. The asymptotic formula

In this section we derive and prove an asymptotic representation formula for $w = u_\varepsilon - u$ in analogy with [9] and [15]. Let $\Phi = \Phi(x, t)$ be any solution of

$$\begin{cases} \Phi_t + k_0 \Delta \Phi - f'(u)\Phi = 0, & \text{in } \Omega \times (0, T), \\ \Phi(T) = 0, & \text{in } \Omega. \end{cases} \tag{42}$$

Our main result is the following

Theorem 5.1. *Assume (2) and (6)–(8). Let u^ε and u be the solutions to (5) and (1) and Φ a solution to (42), respectively. Then, there exist a sequence ω_{ε_n} satisfying β) and*

(4) with $|\omega_{\varepsilon_n}| \to 0$, a regular Borel measure μ and a symmetric matrix $\mathcal{M}$ with elements $\mathcal{M}_{ij} \in L^2(\Omega, \mathrm{d}\mu)$ such that, for $\varepsilon \to 0$,

$$\int_0^T \int_{\partial\Omega} k_0 \frac{\partial \Phi}{\partial n}(u^\varepsilon - u)\mathrm{d}\sigma\mathrm{d}t = |\omega_{\varepsilon_n}| \left\{ \int_0^T \int_\Omega \left(\tilde{k}\mathcal{M}\nabla u \cdot \nabla\Phi + f(u)\Phi \right) \mathrm{d}\mu\mathrm{d}t + o(1) \right\}. \tag{43}$$

To prove theorem 5.1, we need to state some preliminary results. Let $v_\varepsilon^{(j)}$ and $v^{(j)}$ be the variational solutions (depending only on $x \in \Omega$) to the problems

$$(PV_\varepsilon) \begin{cases} \mathrm{div}(k_\varepsilon \nabla v_\varepsilon^{(j)}) = 0, & \text{in } \Omega, \\ \frac{\partial v_\varepsilon^{(j)}}{\partial n} = n_j, & \text{on } \partial\Omega, \\ \int_{\partial\Omega} v_\varepsilon^{(j)} \mathrm{d}\sigma = 0, \end{cases} \quad (PV_0) \begin{cases} \mathrm{div}(k_0 \nabla v^{(j)}) = 0, & \text{in } \Omega, \\ \frac{\partial v^{(j)}}{\partial n} = n_j, & \text{on } \partial\Omega, \\ \int_{\partial\Omega} v^{(j)} \mathrm{d}\sigma = 0, \end{cases} \tag{44}$$

n_j being the jth coordinate of the outward normal to $\partial\Omega$. It can be easily verified that

$$v^{(j)} = x_j - \frac{1}{|\partial\Omega|} \int_{\partial\Omega} x_j \mathrm{d}\sigma. \tag{45}$$

The following results hold

Proposition 5.1. *Let $v_\varepsilon^{(j)}$ and $v^{(j)}$ solutions to (44), then there exists $C(\Omega) > 0$ such that*

$$\|v_\varepsilon^{(j)} - v^{(j)}\|_{H^1(\Omega)} \leqslant C(\Omega)|\omega_\varepsilon|^{\frac{1}{2}}. \tag{46}$$

Moreover, for some $\eta \in (0, \frac{1}{2})$, there exists $C(\Omega, \eta) > 0$ such that

$$\|v_\varepsilon^{(j)} - v^{(j)}\|_{L^2(\Omega)} \leqslant C(\Omega, \eta)|\omega_\varepsilon|^{\frac{1}{2}+\eta}. \tag{47}$$

Proof. See lemma 1 in [15]. □

Proposition 5.2. *Let u and u^ε be the solutions to problems (1) and (5), respectively. Consider $v_\varepsilon^{(j)}$ and $v^{(j)}$ as in (44). Then, $\forall\, \Phi \in C^1(\overline{\Omega} \times [0, T])$ s.t. $\Phi(x, T) = 0$, it holds*

$$\int_0^T \int_\Omega \frac{1}{|\omega_\varepsilon|} \chi_{\omega_\varepsilon} \nabla u \cdot \nabla v_\varepsilon^{(j)} \Phi \mathrm{d}x\mathrm{d}t = \int_0^T \int_\Omega \frac{1}{|\omega_\varepsilon|} \chi_{\omega_\varepsilon} \nabla u^\varepsilon \cdot \nabla v^{(j)} \Phi \mathrm{d}x\mathrm{d}t + o(1), \quad \varepsilon \to 0. \tag{48}$$

Proof. See appendix A.1 in the appendix.

Proof of theorem 5.1. Following [15, section 3], there exist a regular Borel measure μ, a symmetric matrix $\mathcal{M}$ with elements $\mathcal{M}_{ij} \in L^2(\Omega, \mathrm{d}\mu)$, a sequence ω_{ε_n} with $|\omega_{\varepsilon_n}| \to 0$ such that

$$|\omega_{\varepsilon_n}|^{-1} \chi_{\omega_{\varepsilon_n}} \mathrm{d}x \to \mathrm{d}\mu, \qquad |\omega_{\varepsilon_n}|^{-1} \chi_{\omega_{\varepsilon_n}} \frac{\partial v_{\varepsilon_n}^{(j)}}{\partial x_i} \mathrm{d}x \to \mathcal{M}_{ij} \mathrm{d}\mu, \tag{49}$$

in the weak* topology of $C^0(\overline{\Omega})$. On account of (11), we deduce also

$$|\omega_{\varepsilon_n}|^{-1} \chi_{\omega_{\varepsilon_n}} \frac{\partial u(t)}{\partial x_i} \frac{\partial v_{\varepsilon_n}^{(j)}}{\partial x_i} \mathrm{d}x \to \mathcal{M}_{ij} \frac{\partial u(t)}{\partial x_i} \mathrm{d}\mu, \quad \forall\, t \in (0, T), \tag{50}$$

in the weak* topology of $C^0(\overline{\Omega})$. Moreover, recalling (11), (22) and (45), we get

$$\left| \int_0^T \mathrm{d}t \int_\Omega \frac{\chi_{\omega_{\varepsilon_n}}}{|\omega_{\varepsilon_n}|} \frac{\partial u^{\varepsilon_n}}{\partial x_i} \frac{\partial v^{(j)}}{\partial x_i} \mathrm{d}x \right| \leqslant C, \tag{51}$$

where C is independent of ε_n. Hence

$$|\omega_{\varepsilon_n}|^{-1} \chi_{\omega_{\varepsilon_n}} \frac{\partial u^{\varepsilon_n}}{\partial x_i} \frac{\partial v^{(j)}}{\partial x_i} \mathrm{d}x\mathrm{d}t \to \mathrm{d}\nu_j \tag{52}$$

in the weak* topology of $C^0(\overline{\Omega} \times [0,T])$. Combining (48), (50) and (52) we obtain

$$\mathrm{d}\nu_j = \mathcal{M}_{ij} \frac{\partial u(t)}{\partial x_i} \mathrm{d}\mu, \quad \forall\, t \in (0,T). \tag{53}$$

Now, let us multiply the first equation in (42) by w and the first equation in (28) by Φ. Integrating on $\Omega \times (0,T)$ and then by parts, we get

$$\int_0^T \int_\Omega \Phi_t w \mathrm{d}x\mathrm{d}t + \int_0^T \int_\Omega k_0 \nabla\Phi \cdot \nabla w \mathrm{d}x\mathrm{d}t - \int_0^T \int_\Omega f'(u)\Phi w \mathrm{d}x\mathrm{d}t + \int_0^T \int_{\partial\Omega} k_0 \frac{\partial \Phi}{\partial n} w \mathrm{d}\sigma\mathrm{d}t = 0,$$

and

$$\begin{aligned} &\int_0^T \int_\Omega w_t \Phi \mathrm{d}x\mathrm{d}t + \int_0^T \int_\Omega k_0 \nabla w \cdot \nabla\Phi \mathrm{d}x\mathrm{d}t + \int_0^T \int_\Omega \chi_{\Omega/\omega_\varepsilon} p_\varepsilon w \Phi \mathrm{d}x\mathrm{d}t \\ &= \int_0^T \int_{\omega_\varepsilon} \widetilde{k} \nabla u^\varepsilon \cdot \nabla\Phi \mathrm{d}x\mathrm{d}t + \int_0^T \int_{\omega_\varepsilon} f(u)\Phi \mathrm{d}x\mathrm{d}t. \end{aligned}$$

Summing up the two previous equations, we have

$$\begin{aligned} &\int_0^T \int_\Omega (w_t\Phi + \Phi_t w)\mathrm{d}x\mathrm{d}t - \int_0^T \int_\Omega f'(u)\Phi w \mathrm{d}x\mathrm{d}t + \int_0^T \int_{\partial\Omega} k_0 \frac{\partial\Phi}{\partial n} w \mathrm{d}\sigma\mathrm{d}t \\ &+ \int_0^T \int_\Omega \chi_{\Omega/\omega_\varepsilon} p_\varepsilon w \Phi \mathrm{d}x\mathrm{d}t = \int_0^T \int_{\omega_\varepsilon} \widetilde{k} \nabla u^\varepsilon \cdot \nabla\Phi \mathrm{d}x\mathrm{d}t + \int_0^T \int_{\omega_\varepsilon} f(u)\Phi \mathrm{d}x\mathrm{d}t. \end{aligned} \tag{54}$$

Observe that the following identities hold

$$\begin{aligned} &\int_0^T \int_\Omega (w_t\Phi + \Phi_t w)\mathrm{d}x\mathrm{d}t \\ &= \int_\Omega (\Phi(T)w(T) - \Phi(0)w(0))\,\mathrm{d}x - \int_0^T \int_\Omega \Phi w_t \mathrm{d}x\mathrm{d}t + \int_0^T \int_\Omega \Phi w_t \mathrm{d}x\mathrm{d}t = 0, \end{aligned} \tag{55}$$

and then, from (54) we infer

$$\begin{aligned} &\int_0^T \int_\Omega \big(\chi_{\Omega/\omega_\varepsilon} p_\varepsilon w\Phi - f'(u)\Phi w\big)\mathrm{d}x\mathrm{d}t + \int_0^T \int_{\partial\Omega} k_0 \frac{\partial\Phi}{\partial n} w \mathrm{d}\sigma\mathrm{d}t \\ &= \int_0^T \int_{\omega_\varepsilon} \widetilde{k} \nabla u^\varepsilon \cdot \nabla\Phi \mathrm{d}x\mathrm{d}t + \int_0^T \int_{\omega_\varepsilon} f(u)\Phi \mathrm{d}x\mathrm{d}t. \end{aligned} \tag{56}$$

Moreover, on account of (22), we have

$$\begin{aligned}
&\int_0^T \int_\Omega \left(\chi_{\Omega/\omega_\varepsilon} p_\varepsilon w\Phi - f'(u)\Phi w\right) \mathrm{d}x\mathrm{d}t \\
&= \int_0^T \int_\Omega \left(\chi_{\Omega/\omega_\varepsilon} p_\varepsilon w\Phi - \chi_{\Omega/\omega_\varepsilon} f'(u)\Phi w\right) \mathrm{d}x\mathrm{d}t - \int_0^T \int_{\omega_\varepsilon} f'(u)\Phi w \mathrm{d}x\mathrm{d}t \\
&= \int_0^T \int_\Omega \chi_{\Omega/\omega_\varepsilon} (p_\varepsilon - f'(u)) w\Phi \mathrm{d}x\mathrm{d}t + o(|\omega_\varepsilon|) = o(|\omega_\varepsilon|). \qquad (57)
\end{aligned}$$

The last equality in (57) is a consequence of the regularity of f (see (24), from which $|p_\varepsilon - f'(u)| \leqslant C|w|$ follows) and (22). Combining (56) and (57) we obtain

$$\int_0^T \int_{\partial\Omega} k_0 \frac{\partial\Phi}{\partial n} w \mathrm{d}\sigma\mathrm{d}t = |\omega_\varepsilon| \int_0^T \int_\Omega \left(\widetilde{k}|\omega_\varepsilon|^{-1} \chi_{\omega_\varepsilon} \nabla u^\varepsilon \cdot \nabla\Phi + \chi_{\omega_\varepsilon} |\omega_\varepsilon|^{-1} f(u)\Phi\right) \mathrm{d}x\mathrm{d}t + o(|\omega_{\varepsilon_n}|).$$

And finally, by means of (49), (52) and (53), formula (43) holds.

Remark 5.1. We highlight that, with minor changes, the asymptotic expansion (43) extends to the case of piecewise smooth anisotropic conductivities of the form

$$\mathbb{K}_\varepsilon = \begin{cases} \mathbb{K}_0 & \text{in } \Omega \setminus \omega_\varepsilon, \\ \mathbb{K}_1 & \text{in } \omega_\varepsilon, \end{cases} \qquad (58)$$

where $\mathbb{K}_0, \mathbb{K}_1 \in C^\infty(\Omega)$ are symmetric matrix valued functions satisfying

$$\alpha_0|\boldsymbol{\xi}|^2 \leqslant \boldsymbol{\xi}^T \mathbb{K}_0(x)\boldsymbol{\xi} \leqslant \beta_0|\boldsymbol{\xi}|^2, \quad \alpha_1|\xi|^2 \leqslant \boldsymbol{\xi}^T \mathbb{K}_1(x)\boldsymbol{\xi} \leqslant \beta_1|\boldsymbol{\xi}|^2, \quad \forall\, \boldsymbol{\xi} \in \mathbb{R}^3, \forall\, x \in \Omega,$$

with $0 < \alpha_1 < \beta_1 < \alpha_0 < \beta_0$. Then, the asymptotic formula (43) becomes

$$\int_0^T \int_{\partial\Omega} \mathbb{K}_0 \nabla\Phi \cdot n(u^\varepsilon - u) \mathrm{d}\sigma\mathrm{d}t = |\omega_\varepsilon| \int_0^T \int_\Omega \left(\mathcal{M}_{ij}(\mathbb{K}_0 - \mathbb{K}_1)_{ik} \frac{\partial u}{\partial x_k} \frac{\partial\Phi}{\partial x_j} + f(u)\Phi\right) \mathrm{d}\mu\mathrm{d}t + o(|\omega_\varepsilon|)$$

where Φ solves

$$\begin{cases} \Phi_t + \operatorname{div}(\mathbb{K}_0 \nabla\Phi) - f'(u)\Phi = 0, & \text{in } \Omega \times (0,T), \\ \Phi(T) = 0, & \text{in } \Omega, \end{cases} \qquad (59)$$

and u is the background solution of

$$\begin{cases} u_t - \operatorname{div}(\mathbb{K}_0 \nabla u) + f(u) = 0, & \text{in } \Omega \times (0,T), \\ \mathbb{K}_0 \nabla u \cdot n = 0, & \text{on } \partial\Omega \times (0,T), \\ u(0) = 0, & \text{in } \Omega. \end{cases} \qquad (60)$$

The matrix $\mathcal{M}$ is called the polarization tensor associated to the inhomogeneity ω_ε. Indeed, all the results of the previous sections can be extended to the case of constant anisotropic coef-
ficients using for instance the regularity results contained in [33].

Remark 5.2. Let us observe that the asymptotic expansion derived in theorem 5.1 can be extended to the case of a finite number of small well-separated inhomogeneities. Compare section 6 of [9] for the elliptic case.

6. A reconstruction algorithm

We now take advantage of the asymptotic expansion (43) to set a numerical reconstruction procedure for the inverse problem of detecting a spherical inhomogeneity ω_ε from boundary measurements of the electric potential. Following the approach of [10, 17] but taking now into account the time-dependent nature of the problem, we introduce the mismatch functional

$$J(\omega_\varepsilon) = \frac{1}{2}\int_0^T \int_{\partial\Omega} (u^\varepsilon - u_{\text{meas}})^2 \mathrm{d}\sigma\mathrm{d}t, \tag{61}$$

where u^ε is the solution of the perturbed problem (5) in presence of an inclusion ω_ε satisfying hypotheses (3) and (4). Then, the inverse problem can be reformulated as the following minimization problem

$$J(\omega_\varepsilon) \to \min \tag{62}$$

among all the small inclusions, well separated from the boundary. We introduce the following additional assumption on the exact inclusion

$$\omega_\varepsilon = z + \varepsilon B = \{x \in \Omega \text{ s.t. } x = z + \varepsilon b,\ b \in B\}, \tag{63}$$

where $z \in \Omega$ and B is an open, bounded, regular set containing the origin. We remark that we prescribe the geometry of the inclusion to be fixed throughout the whole observation time. The restriction of the functional J to the class of inclusions satisfying (63) is denoted by $j(\varepsilon; z)$. We can now define the *topological gradient* $G : \Omega \to \mathbb{R}$ of j as the first order term appearing in the asymptotic expansion of the cost functional with respect to ε, namely

$$j(\varepsilon; z) = j(0) + |\omega_\varepsilon| G(z) + o(|\omega_\varepsilon|), \quad \varepsilon \to 0, \tag{64}$$

where $j(0) = \int_0^T \int_{\partial\Omega} (u - u_{\text{meas}})^2 \mathrm{d}\sigma\mathrm{d}t$ and u is the solution of the unperturbed problem (1). Observe that $j(0)$ does not depend[5] on z.

Under the assumptions that the exact inclusion has small size and satisfies hypothesis (63), a reconstruction procedure consists in identifying the point $\bar{z} \in \Omega$ where the topological gradient G attains its minimum. Indeed, the cost functional achieves the smallest value when it is evaluated in the center of the exact inclusion. Thanks to the hypothesis of small size, we expect the reduction of the cost functional j to be correctly described by the first order term G, up to a remainder which is negligible with respect to ε.

Nevertheless, in order to define a reconstruction algorithm, the efficient evaluation of the topological gradient G is required. According to the definition above,

$$G(z) = \lim_{\varepsilon \to 0} \frac{j(\varepsilon; z) - j(0)}{|\omega_\varepsilon|}.$$

Evaluating G in a single point $z \in \Omega$ would require to solve the direct problem several times in presence of inclusions centered at z with decreasing volume. This procedure can be indeed avoided thanks to a useful *representation formula* that can be deduced from the asymptotic expansion (43). To show this latter, we need the following preliminary

[5] Indeed, the cost functional achieves the smallest value when it is evaluated in the center of the exact inclusion. This explains why, thanks to (64), the minimum of G will occur at approximately the same location as the minimum of $j(\varepsilon; z)$, when ε is small.

Proposition 6.1. *Consider the problem*

$$\begin{cases} \Phi_t + k_0 \Delta \Phi - f'(u)\Phi = 0, & \text{in } \Omega \times (0,T), \\ \frac{\partial \Phi}{\partial n} = u^\varepsilon - u, & \text{on } \partial\Omega \times (0,T), \\ \Phi(T) = 0, & \text{in } \Omega. \end{cases} \tag{65}$$

Given a compact set $K \subset \Omega$ such that $d(K, \partial\Omega) \geqslant d_0 > 0$ the following estimate holds

$$\|\Phi\|_{L^1(0,T;W^{1,\infty}(K))} \leqslant C \|u^\varepsilon - u\|_{L^2(0,T;L^2(\partial\Omega))}. \tag{66}$$

Proof. See appendix A.2 in the appendix.

By proposition 6.1, we deduce a representation formula for the topological gradient by introducing a suitable *adjoint problem*, according to the following:

Proposition 6.2. *The topological gradient of the cost functional $j(\varepsilon, z)$ can be expressed by*

$$G(z) = \int_0^T \left(\widetilde{k}\mathcal{M}\nabla u(z) \cdot \nabla W(z) + f(u(z))W(z) \right) \mathrm{d}t, \tag{67}$$

where W is the solution of the adjoint problem:

$$\begin{cases} W_t + k_0 \Delta W - f'(u)W = 0, & \text{in } \Omega \times (0,T), \\ k_0 \frac{\partial W}{\partial n} = u - u_{\text{meas}}, & \text{on } \partial\Omega \times (0,T), \\ W(T) = 0, & \text{in } \Omega. \end{cases} \tag{68}$$

Proof. Consider the difference

$$\begin{aligned} j(\varepsilon; z) - j(0) &= \frac{1}{2}\|u^\varepsilon - u_{\text{meas}}\|^2_{L^2(0,T;L^2(\partial\Omega))} - \frac{1}{2}\|u - u_{\text{meas}}\|^2_{L^2(0,T;L^2(\partial\Omega))} \\ &= \int_0^T \int_{\partial\Omega} (u^\varepsilon - u)(u - u_{\text{meas}}) \mathrm{d}\sigma \mathrm{d}t + \frac{1}{2}\|u^\varepsilon - u\|^2_{L^2(0,T;L^2(\partial\Omega))}. \end{aligned} \tag{69}$$

According to (43) and to the definition of the adjoint problem (68), we can express

$$\int_0^T \int_{\partial\Omega} (u^\varepsilon - u)(u - u_{\text{meas}}) \mathrm{d}\sigma \mathrm{d}t = |\omega_\varepsilon| \left\{ \int_0^T \int_\Omega \widetilde{k}\mathcal{M}\nabla u \cdot \nabla W \mathrm{d}\mu \mathrm{d}t + \int_0^T \int_\Omega f(u) W \mathrm{d}\mu \mathrm{d}t + o(1) \right\}.$$

Since we assume (63), the measure μ associated to the inclusion is the Dirac mass δ_z centered in point z (see [15]). Hence

$$\int_0^T \int_{\partial\Omega} (u^\varepsilon - u)(u - u_{\text{meas}}) \mathrm{d}\sigma \mathrm{d}t = |\omega_\varepsilon| \int_0^T \left\{ \widetilde{k}\mathcal{M}\nabla u(z) \cdot \nabla W(z) + f(u(z))W(z) \right\} \mathrm{d}t + o(|\omega_\varepsilon|). \tag{70}$$

Moreover, by (43), the second term in the left-hand side of (69) can be expressed as

$$\int_0^T \int_{\partial\Omega} (u^\varepsilon - u)(u^\varepsilon - u) \mathrm{d}\sigma \mathrm{d}t = |\omega_\varepsilon| \int_0^T \left\{ \widetilde{k}\mathcal{M}\nabla u(z) \cdot \nabla \Phi(z) + f(u(z))\Phi(z) \right\} \mathrm{d}t + o(|\omega_\varepsilon|),$$

where Φ is the solution to (65). Thanks to regularity results on u (see theorem 3.1) and using proposition 6.1 with $K = \Omega_{d_0} = \{x \in \Omega s.t. d(x, \partial\Omega) \geqslant d_0\}$, we obtain

$$\begin{aligned}
&\int_0^T \int_{\partial\Omega} (u^\varepsilon - u)(u^\varepsilon - u) \mathrm{d}\sigma \mathrm{d}t \leqslant C|\omega_\varepsilon| \left\{ \int_0^T |\nabla\Phi(z)| \mathrm{d}t + \int_0^T |\Phi(z)| \mathrm{d}t \right\} + o(|\omega_\varepsilon|) \\
&\leqslant C|\omega_\varepsilon| \|u^\varepsilon - u\|_{L^2(0,T,L^2(\partial\Omega))} + o(|\omega_\varepsilon|) \leqslant C|\omega_\varepsilon| \|u^\varepsilon - u\|_{L^2(0,T,H^1(\Omega))} + o(|\omega_\varepsilon|) \\
&\leqslant C|\omega_\varepsilon|^{\frac{3}{2}} + o(|\omega_\varepsilon|) = o(|\omega_\varepsilon|).
\end{aligned} \tag{71}$$

Replacing (70) and (71) in (69), we finally get

$$j(\varepsilon; z) - j(0) = |\omega_\varepsilon| \left\{ \int_0^T \widetilde{k}\mathcal{M}\nabla u(z) \cdot \nabla W(z) \mathrm{d}t + \int_0^T f(u(z)) W(z) \mathrm{d}t \right\} + o(|\omega_\varepsilon|).$$

Thanks to the representation formula (67), evaluating the topological gradient of the cost functional requires just the solution of two initial and boundary value problems. This yields the definition of a *one-shot algorithm* for the identification of the center of a small inclusion satisfying hypotesis (63) (see algorithm 1).

Algorithm 1. Reconstruction of a single inclusion of small dimensions.

Require: $u_0(x, 0)\ \forall\, x \in \Omega$, $u_{\text{meas}}(x, t)\ \forall\, x \in \partial\Omega, t \in (0, T)$.
Ensure: approximated centre of the inclusion, $\bar{z}$

1. compute u by solving (1);
2. compute W by solving (68);
3. determine G according to (67);
4. find $\bar{z}$ s.t. $G(\bar{z}) \leqslant G(z) \quad \forall\, z \in \Omega$.

Guided by the application in electrophysiological we have in mind, we consider also the case of *partial boundary measurements* where the support of u_{meas} is given by a subset $\Gamma \subset \partial\Omega$. In this case, it is possible to formulate a slightly different optimization problem than (62), in which the mismatch $u^\varepsilon - u_{\text{mean}}$ is minimized just on the portion Γ of the boundary. The same reconstruction algorithm can be devised for this problem by simply considering nonhomogeneous Neumann conditions in the adjoint problem (65) only on Γ.

7. Numerical results

We rely on the Galerkin finite element method for the numerical approximation of the background problem (1) and the adjoint problem (68), as well as to compute the solution to the perturbed problem (5) in presence of the exact inclusion when considering synthetic data u_{meas}. The one-shot procedure makes the reconstruction algorithm very efficient, only requiring the solution of an adjoint problem for each acquired measurement over the time interval, without entailing any iterative (e.g. descent) method for numerical optimization.

7.1. Finite element approximation

The background problem (1) can be cast in weak form as follows: $\forall\, t \in (0, T)$, *find* $u(t) \in V = H^1(\Omega)$ *such that* $u(0) = u_0$ *and*

Table 1. Numerical values of physical coefficients.

ν	C_m	A^2	u_1	u_2	u_3	k_f^i	k_t^i	k_r^i	k_f^e	k_t^e	k_r^e
500 m A^{-1}	0.1 mA ms cm^{-2}	0.2	0	0.15	1	3	1	0.315	2	1.65	1.351

$$\int_\Omega u_t v \mathrm{d}x + \int_\Omega k_1 \nabla u \cdot \nabla v \mathrm{d}x + \int_\Omega f(u) v \mathrm{d}x = 0, \qquad \forall\, v \in V. \tag{72}$$

By introducing a finite-dimensional subspace V_h of V, $\dim(V_h) = N_h < \infty$, the Galerkin (semi-discretized in space) formulation of problem (72) reads: $\forall\, t \in (0,T)$, *find* $u_h(t) \in V_h$ *such that* $u_h(0) = u_{h,0}$ *and*

$$\int_\Omega (u_h)_t v_h \mathrm{d}x + b(u_h(t), v_h) + F(u_h(t), v_h) = 0, \qquad \forall\, v_h \in V_h, \tag{73}$$

where $b(u,v) = \int_\Omega k_1 \nabla u \cdot \nabla v \mathrm{d}x$, $F(u,v) = \int_\Omega f(u) v \mathrm{d}x$, f is defined as in (2) and $u_{h,0}$ is the H^1-projection of u_0 onto V_h.

To obtain a full discretization of the problem, we introduce a finite difference approximation in time. According to the strategy reported in [20], we rely on a semi-implicit scheme which allows an efficient treatment of the nonlinear terms. Let us consider an uniform partition $\{t^n\}_{n=0}^N$ of the time interval $[0,T]$ of step $\tau = \frac{T}{N}$ s.t. $t^0 = 0$, $t^N = T$. Then, the fully discrete formulation of (1) is given by: $\forall\, n = 0, \dots N-1$, *find* $u_h^{n+1} \in V_h$ *such that* $u_h^0 = u_{0,h}$ *and*

$$\int_\Omega u_h^{n+1} v_h \mathrm{d}x - \int_\Omega u_h^n v_h \mathrm{d}x + \tau b(u_h^{n+1}, v_h) + \tau F(u_h^n, v_h) = 0, \qquad \forall\, v_h \in V_h. \tag{74}$$

With the same discretization strategy one may describe a numerical scheme for the approximate solution of the perturbed problem, using the weak form reported in (14) and introducing the forms

$$b_\varepsilon(u,v) = \int_\Omega k_\varepsilon \nabla u \cdot \nabla v \mathrm{d}x, \qquad F_\varepsilon(u,v) = \int_\Omega \chi_{\Omega \setminus \omega_\varepsilon} f(u) v \mathrm{d}x.$$

The adjoint problem, instead, requires the introduction of the form $\mathrm{d}F(u,v;w) = \int_\Omega f'(w) u v \mathrm{d}x$, which is bilinear with respect to u and v. Thanks to the linearity of the adjoint problem, we can consider a fully implicit Crank–Nicolson scheme: $\forall\, n = 0, \dots N-1$, *find* $w_h^n \in V = H^1(\Omega)$ *such that* $w_h^N = 0$ *and*

$$\begin{aligned} \int_\Omega w_h^{n+1} v_h \mathrm{d}x - \int_\Omega w_h^n v_h \mathrm{d}x + \frac{\tau}{2} \big(& b(w_h^{n+1}, v_h) + b(w_h^n, v_h) \\ & + \mathrm{d}F(w_h^{n+1}, v_h; u_h^{n+1}) + \mathrm{d}F(w_h^n, v_h; u_h^n) \big) \\ = \frac{\tau}{2} & \left(\int_{\partial\Omega} (u_h^{n+1} - u_{\mathrm{meas}}(t^{n+1})) v_h \mathrm{d}\sigma + \int_{\partial\Omega} (u_h^n - u_{\mathrm{meas}}(t^n)) v_h \mathrm{d}\sigma \right), \quad \forall\, v_h \in V_h. \end{aligned} \tag{75}$$

Existence and uniqueness of the solution to the fully-discrete problems (74) and (75) follow by the well-posedness of the continuous problems, since V_h is a subspace of $H^1(\Omega)$; see, e.g. [25, 46] and [20] for a detailed stability and convergence analysis of the proposed schemes.

The numerical setup for the simulation is represented in figure 1. We consider an idealized geometry of the left ventricle (which has been object of several studies, see e.g. [20]), and define a tetrahedral tesselation $\mathcal{T}_h$ of the domain. The discrete space V_h is the P1-finite element

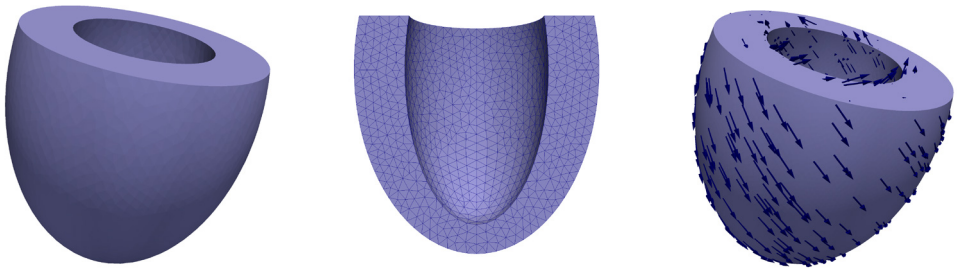

(a) (b) (c)

Figure 1. Setup of numerical test cases. (a) Domain. (b) Mesh (section). (c) Fiber directions.

space over $\mathcal{T}_h$, i.e. the space of the continuous functions over Ω which are linear polynomials when restricted on each element $T \in \mathcal{T}_h$. The mesh we use for all the reported results consists of 24 924 tetrahedric elements and $N_h = 5639$ nodes. We report also the anisotropic structure considered in all the recontruction tests, according to [42, 44] and [20]. The conductivity matrix $\mathbb{K}_0$ for the monodomain equation is given by $\mathbb{K}_0(x) = \mathbb{K}^e(x)(\mathbb{K}^e(x) + \mathbb{K}^i(x))^{-1}\mathbb{K}^i(x)$, where $\mathbb{K}^i$ and $\mathbb{K}^e$ are orthotropic tensors with three constant positive real eigenvalues, namely

$$\mathbb{K}^e(x) = k_f^e \vec{e_f}(x) \otimes \vec{e_f}(x) + k_t^e \vec{e_t}(x) \otimes \vec{e_t}(x) + k_r^e \vec{e_r}(x) \otimes \vec{e_r}(x)$$
$$\mathbb{K}^i(x) = k_f^i \vec{e_f}(x) \otimes \vec{e_f}(x) + k_t^i \vec{e_t}(x) \otimes \vec{e_t}(x) + k_r^i \vec{e_r}(x) \otimes \vec{e_r}(x).$$

The eigenvectors $\vec{e_f}$, $\vec{e_t}$ and $\vec{e_r}$ are associated to the three principal directions of conductivity in the heart tissue: respectively, the fiber centerline, the tangent direction to the heart sheets and the transmural direction (normal to the sheets).

For the direct problem simulations, we consider the formulation reported in (1), specifying realistic values for the parameters C_m and ν. We have rescaled the values of u_1, u_2, u_3 and A^2 in order to simulate the electric potential in the adimensional range $[0, 1]$. The rescaling is given by $\tilde{u} = (\alpha + u)/\beta$, where $\alpha = 0.085$ mV and $\beta = 0.125$ mV, whereas for the sake of simplicity we will still denote by u the rescaled variable $\tilde{u}$. We consider the initial datum u_0 to be positive on a band of the endocardium, representing the initial stimulus provided by the heart conducting system. The most relevant parameters, chosen according to [27, 47], are reported in table 1.

In figure 2 we report the solution of the discrete background problem (74) at different time instants, comparing the isotropic and the anisotropic cases.

7.2. Reconstruction of small inclusions

We now tackle the problem of reconstructing the position of a small inhomogeneity using the knowledge of the electric potential on a portion Γ of the boundary. In particular, we assume that u_{meas} is known on the endocardium, i.e. the inner surface of the heart cavity. In each numerical experiment, we consider the presence of a spherical inclusion of small size (the ratio $\rho_{\text{isch}}/\rho_{ventr}$ between the radius of the inhomogeneity and the radius of the horizontal section of the ventricle is 0.05) and consider a contrast of two orders of magnitude in the conductivity tensor between the ischemic and healthy tissue: $\mathbb{K}_1 = 0.01 \cdot \mathbb{K}_0$. We generate synthetic data on a more refined mesh and test the effectiveness of algorithm 1 in the reconstruction of a small spherical inclusion in different positions. In figure 3 we report the value of the topological gradient and superimpose the exact inclusions (that is, the ones corresponding to the conductivity

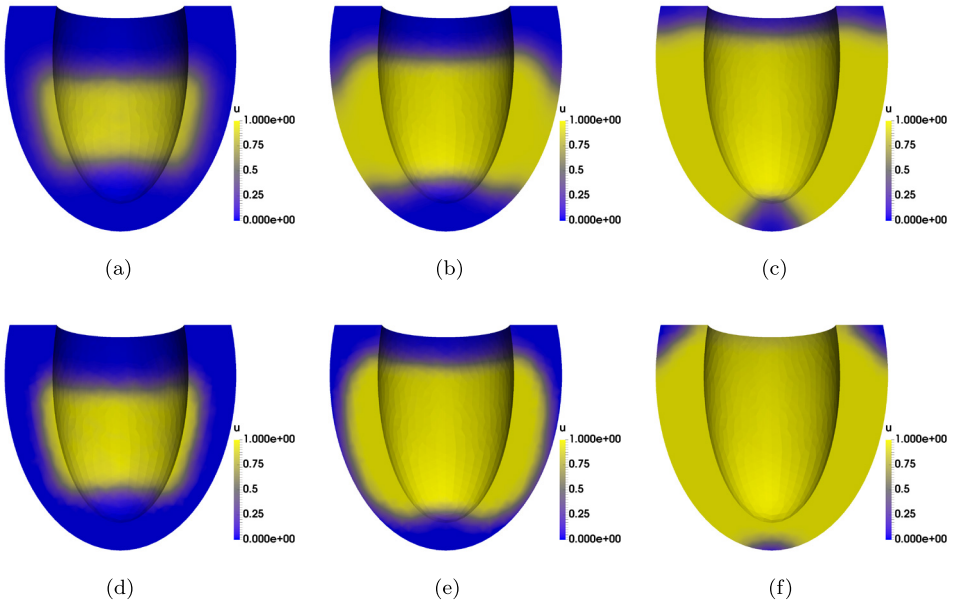

Figure 2. Background problem simulation: isotropic case (top) and anisotropic case (bottom) at different time instants. (a) Isotropic case, $t = 0.2$ T. (b) Isotropic case, $t = 0.5$ T. (c) Isotropic case, $t = 0.8$ T. (d) Anisotropic case, $t = 0.2$ T (e) Anisotropic case, $t = 0.5$ T. (f) Anisotropic case, $t = 0.8$ T.

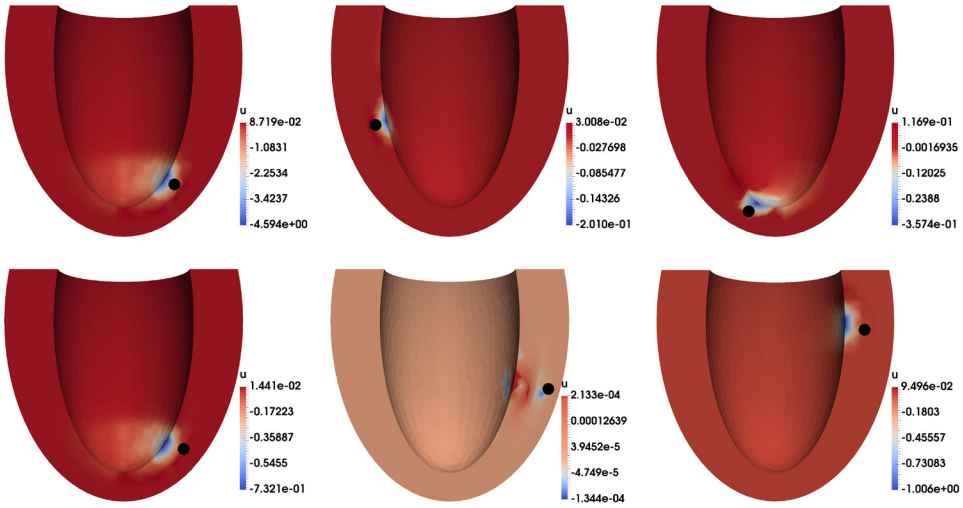

Figure 3. Reconstruction of small inclusions: topological gradient for different configurations.

fields which have generated synthetic data): we observe a negative region in proximity of the position of the real inclusion. The algorithm precisely identifies the region where the inclusion is present, whereas the minimum may in general be found along the endocardium also when the center of the real inclusion is not located on the heart surface. Nevertheless, due to the domain thinness, the reconstructed position is found to be close to the real one.

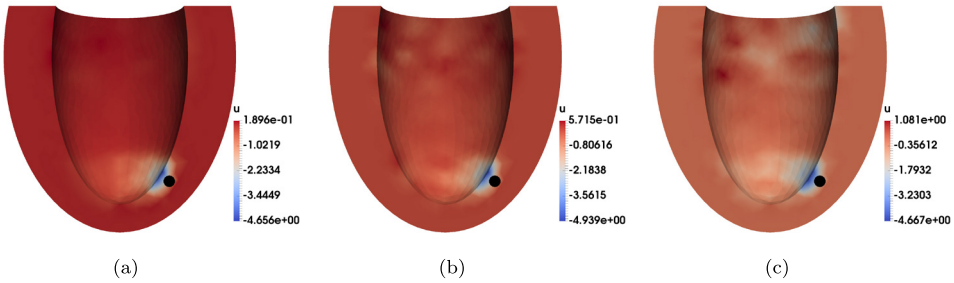

Figure 4. Reconstruction of small inclusions: results in presence of different noise levels. (a) $p = 1\%$. (b) $p = 5\%$. (c) $p = 10\%$.

This slight loss in accuracy seems to be an intrinsic limit of the topological gradient strategy applied to the problem at hand. We point out that the reconstruction is performed by relying on a single measurement acquired on the boundary. This latter is a constraint imposed by the physical problem at hand, for which multiple measurements corresponding to different sources cannot be retrieved. As a matter of fact, all the techniques based on several measurements in order to increase the quality of the reconstruction are impracticable. A different strategy, as proposed in several works focusing on steady problems, may consist in introducing a modification to the cost functional J. In [3] and related works the authors introduce a cost functional inherited from imaging techniques, whereas in [17, 40] different strategies involving the Kohn–Vogelius functional or similar ones are explored. Nevertheless, the nonlinearity of the direct problem considered in this work prevents the possibility to apply these techniques, since the analitycal expressions of the fundamental solution, single and double layer potentials would not be available in practice.

7.3. Reconstruction in presence of experimental noise

We then test the stability of the algorithm in presence of experimental noise on the measured data u_{meas}. We consider different noise levels, according to the formula

$$\widetilde{u}_{\text{meas}}(x,t) = u_{\text{meas}}(x,t) + p\eta(x,t),$$

where $\eta(x,t)$ for each x,t is a Gaussian random variable with zero mean and standard deviation equal to $u_3 - u_1$, whereas $p \in [0,1]$ is the noise level. In figure 4 the results of the reconstruction in presence of different noise levels are compared. The algorithm shows to be robust with respect to large noise levels and increasingly accurate as the noise level reduces.

7.4. Reconstruction from partial discrete data

A further test case to assess at which extent the proposed procedure is effective deals with the reconstruction of small inclusions starting from the knowledge of partial data. These latter are provided by single measurements of the electric potential in a discrete set of points on the endocardium, possibly simulating the procedure of intracavitary electric measurements. Figure 5 shows that the algorithm is able to detect the presence of a small inclusion from the knowledge of the potential on $N_p = 246, 61, 15$ different points, shown in the bottom part of figure 5. The position of the reconstructed inclusion is slightly affected by the reduction of sampling points; nevertheless, reliable reconstructions can be obtained even with a very small (compared to the number of mesh vertices lying on that boundary) number of points.

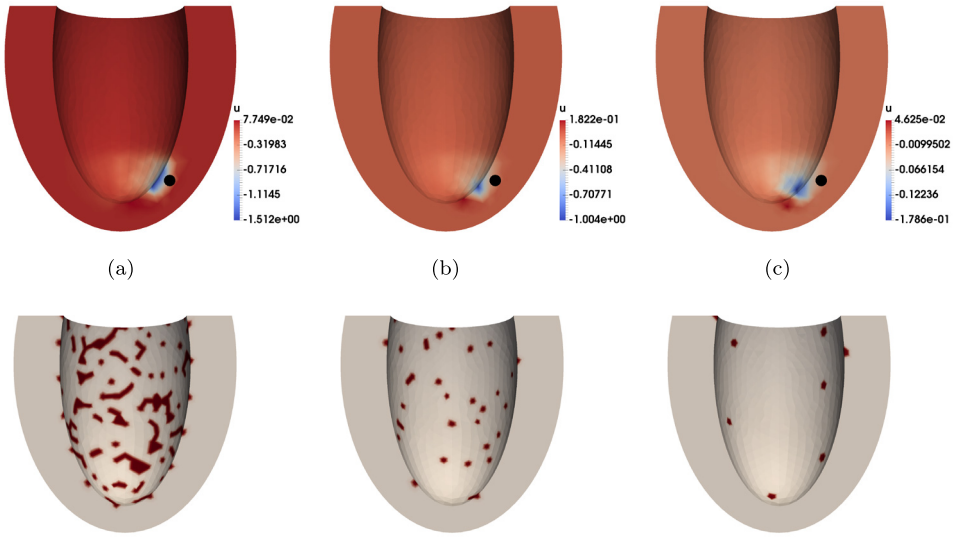

Figure 5. Reconstruction of small inclusions in presence of partial data. Top: topological gradient; bottom: mesh elements containing sampling points. (a) $N_p = 246$. (b) $N_p = 61$. (c) $N_p = 15$.

For the same purpose, we have tested the capability of the reconstruction procedure to avoid *false positives*: the algorithm is able to distinguish the case where inclusions are either present or absent, also in the case where the data are recovered only at a finite set of points, and are affected by noise. We compare the value of the cost functional J and of the minimum of the topological gradient G obtained through algorithm 1 on data generated when (i) a small inclusion is present or (ii) no inclusion is considered. The measurement is performed on a set of $N_p = 100$ points and is affected by different noise levels. The results are reported in table 2.

The presence of a small noise on measured data causes a great increase of J: with 5% noise, e.g. the value of J is two orders of magnitude greater than the value assumed in presence of a small inclusion without noise. Nevertheless, the topological gradient G allows to distinguish the false positive cases, since (at least in the case of small noise level) the value attained by its minimum in presence of a small inclusion is considerably lower than the random oscillations of G due to noise.

7.5. Reconstruction of larger inclusions

We finally assess the performance of algorithm 1, developed for the reconstruction of small inclusions well separated from the boundary, in detecting the position of extended inclusions. This case is of great potential interest in view of the problem of detecting ischemic regions[6]. The most important assumption on which the *one-shot* procedure above relies is that the variation of the cost functional when passing from the background case value ($J(0)$) to the value corresponding to the exact inclusion can be correctly described by the first order term of its

[6] Total occlusion of a major coronary artery generally causes the entire thickness of the ventricular wall to become ischemic (transmural ischemia) or, alternatively, a significant ischemia only in the endocardium, that is, the inner layer of the myocardium (subendocardial ischemia). See, e.g. [19] for a detailed investigation of the interaction between the presence of moderate or severe subendocardial ischemic regions and the anisotropic structure of the cardiac muscle.

Table 2. False positive test. Comparison between reconstructions obtained from data measured in presence of an inclusion (left table) and data measured with no inclusion present (right table). The null results in the first row of table (b) are due to the usage of synthetic data.

(a) Results in presence of an inclusion

Error (%)	N_p	J	$\min_\Omega G$
0	100	0.275	−0.5793
1	100	1.235	−0.589
2	100	4.128	−0.530
5	100	24.429	−0.589

(b) Results with no inclusion present

Error (%)	N_p	J	$\min_\Omega G$
0	100	0.000	0.000
1	100	0.964	−0.044
2	100	3.864	−0.105
5	100	24.148	−0.189

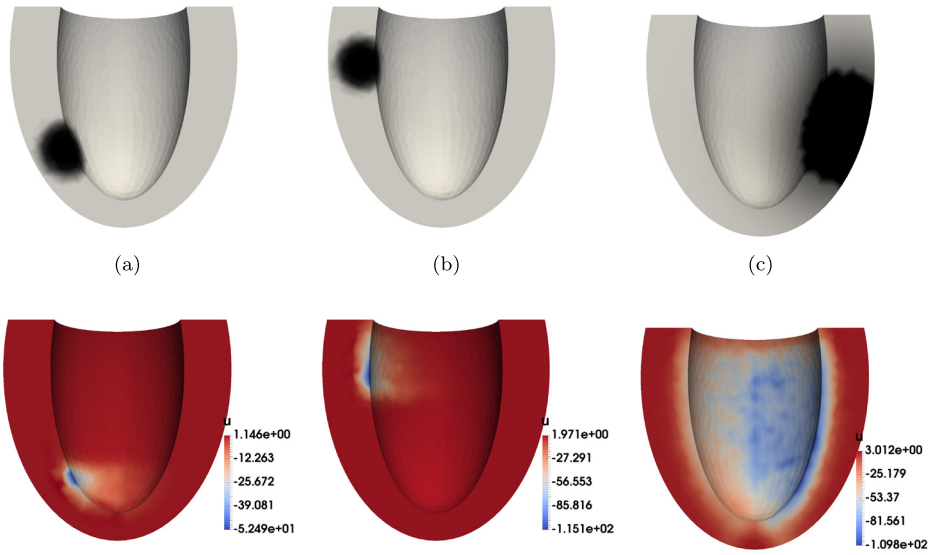

Figure 6. Reconstruction of larger inclusions, with $\rho_{\text{isch}}/\rho_{\text{ventr}} = 0.25$ (left and center plot), $\rho_{\text{isch}}/\rho_{\text{ventr}} = 0.5$ (right plot). Top: exact inclusion; bottom: topological gradient. (a) radius = 1. (b) radius = 1. (c) radius = 2.

asymptotic expansion, namely the topological gradient G. Removing the hypothesis of small size extension, we cannot rigorously assess the accuracy of the algorithm; however, the proposed procedure still allows us to identify the location of the inclusion.

We report the results of some numerical experiments conducted in presence of an inclusion of larger size, i.e. $\rho_{\text{isch}}/\rho_{\text{ventr}} = 0.25$, not even separated from the boundary. As depicted in figure 6, the minimum of the topological gradient is close to the position of the inclusion, and attains lower values with respect to the previously reported cases. When considering very extended ischemic regions (e.g. $\rho_{\text{isch}}/\rho_{\text{ventr}} = 0.5$), though, the information given by the

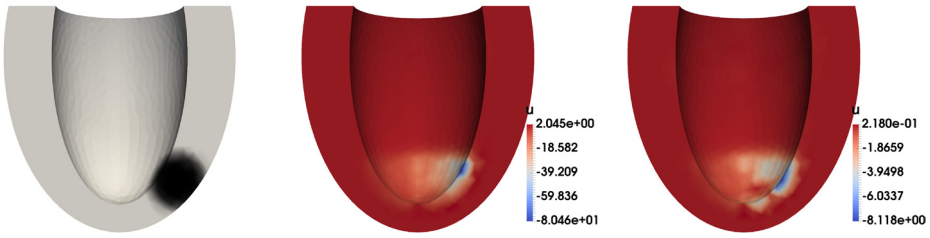

(a) (b) (c)

Figure 7. Larger ischemic regions: stability of the reconstruction. (a) Exact inclusion. (b) Topological gradient, 2% noise. (c) Topological gradient, 2% noise, measurements on 100 points.

topological gradient is less accurate—nevertheless, showing lower values close to the position of the inclusion.

Moreover, in figure 7 we assess the stability of the reconstruction with respect to the presence of noisy data and partial measurements, as done in the case of small inclusions. Also in this case reliable reconstructions can be obtained even in presence of noise, and/or data measured in a small number of points.

8. Conclusions and perspectives

A rigorous theoretical analysis of the inverse problem of detecting inhomogeneities in the monodomain equations has allowed us to set up a numerical reconstruction procedure. The ultimate goal in this respect would be the detection of ischemic regions in the myocardic tissue from a single measurement of the endocardial potential. The identification is made possible by evaluating the topological gradient of a quadratic cost functional, requiring the solution of two initial and boundary value problems, the background problem and the adjoint one. Numerical results are encouraging and allow to estimate the position of the inclusion, although the identified inhomogeneity is nearly always detected on the boundary where the measurement is acquired. Nevertheless, by relying on a single measurement for the sake of identification and on a *one-shot* procedure, the obtained results give useful insights.

Many issues are still open. Concerning the mathematical model, even more interesting cases would be those involving (i) the coupling with an ODE system for modeling the dynamics of the gating variables, so that the whole heartbeat can be simulated; (ii) the heart-torso coupling, so that more realistic (and noninvasive) body surface measurements can be employed; (iii) a bidomain model instead of the monodomain case considered in this paper, to enhance the description of the electrical activity. Setting and analyzing the inverse problem in a context where (at least one of) these features are considered represents the natural continuation of the present work.

Finally, to close the gap between the rigorous mathematical setting and the practice, the two assumptions made in this work about the size of the inclusion and its distance from the boundary should be relaxed. Numerical results shown in section 7.5 provide a first insight on the detection of inclusions with larger size, as those which would correspond to transmural or subendocardial ischemias. From a mathematical standpoint, this problem is still open. Also in the case of a linear direct problem, very few results can be found in literature, see, e.g. [2]. Estimating the size of the inclusion is another open question in the case of parabolic PDEs, also for linear equations. The case of multiple inclusions, addressed in [10] for a stationary nonlinear problem, could also be considered. Last, but not least, the topological optimization

framework addressed in this paper could also be combined with an iterative algorithm, such as the level set method, or with the solution of a successive shape optimization problem, to achieve a full reconstruction both of the dimension and the shape of the inclusion.

Acknowledgments

We acknowledge the use of the MATLAB library [48] for the numerical simulations presented in this work, and we thank Dr Stefano Pagani (EPFL) for his feedback and suggestions. E Beretta, C Cavaterra, M C Cerutti and L Ratti thank the New York University in Abu Dhabi for its kind hospitality that permitted further development of the present research. The work of C Cavaterra was supported by the FP7-IDEAS-ERC-StG 256872 (EntroPhase) and by GNAMPA (Gruppo Nazionale per l'Analisi Matematica, la Probabilità e le loro Applicazioni).

Appendix

We report here the proofs of propositions 6 and 7.

A.1. Proof of proposition 5.2

We follow the ideas in [9] and [15]. Since $w = u^\varepsilon - u$, then we obtain the identity

$$\int_\Omega k_0 \nabla w \cdot \nabla \left(v^{(j)} \Phi \right) \mathrm{d}x = - \int_\Omega k_0 w \nabla v^{(j)} \cdot \nabla \Phi \mathrm{d}x + \int_{\partial\Omega} k_0 w n_j \Phi \mathrm{d}\sigma + \int_\Omega k_0 \nabla w \cdot \nabla \Phi v^{(j)} \mathrm{d}x. \tag{A.1}$$

Moreover, we have

$$\int_0^T \int_\Omega k_\varepsilon \nabla w \cdot \nabla \left(v_\varepsilon^{(j)} \Phi \right) \mathrm{d}x\mathrm{d}t = \int_0^T \int_\Omega k_\varepsilon \left(\nabla w \cdot \nabla v_\varepsilon^{(j)} \Phi + \nabla w \cdot \nabla \Phi v^{(j)} + \nabla w \cdot \nabla \Phi (v_\varepsilon^{(j)} - v^{(j)}) \right) \mathrm{d}x\mathrm{d}t$$

$$= \int_0^T \Big(- \int_\Omega k_\varepsilon w \nabla v_\varepsilon^{(j)} \cdot \nabla \Phi \mathrm{d}x + \int_{\partial\Omega} k_0 w n_j \Phi \mathrm{d}\sigma + \int_\Omega k_0 \nabla w \cdot \nabla \Phi v^{(j)} \mathrm{d}x$$

$$+ \int_\Omega (k_\varepsilon - k_0) \nabla w \cdot \nabla \Phi v^{(j)} \mathrm{d}x + \int_\Omega k_\varepsilon \nabla w \cdot \nabla \Phi (v_\varepsilon^{(j)} - v^{(j)}) \mathrm{d}x \Big) \mathrm{d}t$$

$$= \int_0^T \Big(- \int_\Omega k_\varepsilon w \nabla v^{(j)} \cdot \nabla \Phi \mathrm{d}x + \int_{\partial\Omega} k_0 w n_j \Phi \mathrm{d}\sigma + \int_\Omega k_0 \nabla w \cdot \nabla \Phi v^{(j)} \mathrm{d}x$$

$$+ \int_{\omega_\varepsilon} (k_1 - k_0) \nabla w \cdot \nabla \Phi v^{(j)} \mathrm{d}x + \int_\Omega k_\varepsilon \nabla w \cdot \nabla \Phi (v_\varepsilon^{(j)} - v^{(j)}) \mathrm{d}x - \int_\Omega k_\varepsilon w \nabla (v_\varepsilon^{(j)} - v^{(j)}) \cdot \nabla \Phi \mathrm{d}x \Big) \mathrm{d}t.$$

A combination with (A.1) gives

$$\int_0^T \int_\Omega k_\varepsilon \nabla w \cdot \nabla (v_\varepsilon^{(j)} \Phi) \mathrm{d}x\mathrm{d}t = \int_0^T \Big(\int_\Omega k_0 \nabla w \cdot \nabla \left(v^{(j)} \Phi \right) \mathrm{d}x + \int_{\omega_\varepsilon} (k_1 - k_0) \nabla w \cdot \nabla \Phi v^{(j)} \mathrm{d}x$$

$$+ \int_{\omega_\varepsilon} (k_0 - k_1) w \nabla v^{(j)} \cdot \nabla \Phi \mathrm{d}x + \int_\Omega k_\varepsilon \nabla w \cdot \nabla \Phi (v_\varepsilon^{(j)} - v^{(j)}) \mathrm{d}x - \int_\Omega k_\varepsilon w \nabla (v_\varepsilon^{(j)} - v^{(j)}) \cdot \nabla \Phi \mathrm{d}x \Big) \mathrm{d}t.$$

Then, on account of (20), (21), (46) and (47) and Schwarz inequality, we get

$$\int_0^T \int_\Omega k_\varepsilon \nabla w \cdot \nabla(v_\varepsilon^{(j)}\Phi)\mathrm{d}x\mathrm{d}t = \int_0^T \left(\int_\Omega k_0 \nabla w \cdot \nabla(v^{(j)}\Phi)\mathrm{d}x - \int_{\omega_\varepsilon} \widetilde{k} \nabla w \cdot \nabla\Phi v^{(j)}\mathrm{d}x \right) \mathrm{d}t + o(|\omega_\varepsilon|). \tag{A.2}$$

Let us consider now problems (23) and (28). Multiplying the first equation in (23) by $v_\varepsilon^{(j)}\Phi$ and the first equation in (28) by $v^{(j)}\Phi$, an integration by parts on $\Omega \times (0,T)$ gives

$$\int_0^T \int_\Omega \left[w_t v_\varepsilon^{(j)}\Phi + k_\varepsilon \nabla w \cdot \nabla(v_\varepsilon^{(j)}\Phi) + \chi_{\Omega/\omega_\varepsilon} p_\varepsilon w v_\varepsilon^{(j)}\Phi \right] \mathrm{d}x\mathrm{d}t = \int_0^T \int_{\omega_\varepsilon} \left[\widetilde{k}\nabla u \cdot \nabla(v_\varepsilon^{(j)}\Phi) + f(u) v_\varepsilon^{(j)}\Phi \right] \mathrm{d}x\mathrm{d}t,$$

$$\int_0^T \int_\Omega \left[w_t v^{(j)}\Phi + k_0 \nabla w \cdot \nabla(v^{(j)}\Phi) + \chi_{\Omega/\omega_\varepsilon} p_\varepsilon w v^{(j)}\Phi \right] \mathrm{d}x\mathrm{d}t = \int_0^T \int_{\omega_\varepsilon} \left[\widetilde{k}\nabla u^\varepsilon \cdot \nabla(v^{(j)}\Phi) + f(u) v^{(j)}\Phi \right] \mathrm{d}x\mathrm{d}t.$$

By a combination of the previous three identities we obtain, for $\varepsilon \to 0$,

$$\int_0^T \int_{\omega_\varepsilon} \widetilde{k}\nabla u \cdot \nabla(v_\varepsilon^{(j)}\Phi)\mathrm{d}x\mathrm{d}t + \int_0^T \int_{\omega_\varepsilon} f(u) v_\varepsilon^{(j)}\Phi \mathrm{d}x\mathrm{d}t - \int_0^T \int_\Omega w_t v_\varepsilon^{(j)}\Phi \mathrm{d}x\mathrm{d}t - \int_0^T \int_\Omega \chi_{\Omega/\omega_\varepsilon} p_\varepsilon w v_\varepsilon^{(j)}\Phi \mathrm{d}x\mathrm{d}t$$

$$= \int_0^T \int_{\omega_\varepsilon} \widetilde{k}\nabla u^\varepsilon \cdot \nabla(v^{(j)}\Phi)\mathrm{d}x\mathrm{d}t + \int_0^T \int_{\omega_\varepsilon} f(u) v^{(j)}\Phi \mathrm{d}x\mathrm{d}t - \int_0^T \int_\Omega w_t v^{(j)}\Phi \mathrm{d}x\mathrm{d}t$$

$$- \int_0^T \int_\Omega \chi_{\Omega/\omega_\varepsilon} p_\varepsilon w v^{(j)}\Phi \mathrm{d}x\mathrm{d}t - \int_0^T \int_{\omega_\varepsilon} \tilde{k}\nabla w \cdot \nabla\Phi v^{(j)}\mathrm{d}x\mathrm{d}t + o(|\omega_\varepsilon|),$$

from which we deduce

$$\int_0^T \int_{\omega_\varepsilon} \widetilde{k}\nabla u \cdot \nabla(v_\varepsilon^{(j)}\Phi)\mathrm{d}x\mathrm{d}t = \int_0^T \int_\Omega w_t (v_\varepsilon^{(j)} - v^{(j)})\Phi \mathrm{d}x\mathrm{d}t + \widetilde{k} \int_0^T \int_{\omega_\varepsilon} \left(\nabla u^\varepsilon \cdot \nabla(v^{(j)}\Phi) - \nabla u^\varepsilon \cdot \nabla\Phi v^{(j)} \right) \mathrm{d}x\mathrm{d}t$$

$$+ \int_0^T \int_{\omega_\varepsilon} \widetilde{k}\nabla u \cdot \nabla\Phi v^{(j)}\mathrm{d}x\mathrm{d}t - \int_0^T \int_\Omega \chi_{\Omega/\omega_\varepsilon} p_\varepsilon w (v_\varepsilon^{(j)} - v^{(j)})\Phi \mathrm{d}x\mathrm{d}t + \int_0^T \int_{\omega_\varepsilon} f(u)(v^{(j)} - v_\varepsilon^{(j)})\Phi \mathrm{d}x\mathrm{d}t + o(|\omega_\varepsilon|).$$

By means of (41), (22), (46) and (47), and recalling also (9) and (25), an application of the Hölder inequality both in space and time gives, for $\varepsilon \to 0$,

$$\widetilde{k} \int_0^T \int_{\omega_\varepsilon} \nabla u \cdot \nabla(v_\varepsilon^{(j)}\Phi)\mathrm{d}x\mathrm{d}t = \int_0^T \int_\Omega w_t (v_\varepsilon^{(j)} - v^{(j)})\Phi \mathrm{d}x\mathrm{d}t + \widetilde{k} \int_0^T \int_{\omega_\varepsilon} \left(\nabla u^\varepsilon \cdot \nabla v^{(j)}\Phi \right.$$
$$\left. + \nabla u \cdot \nabla\Phi v^{(j)} \right) \mathrm{d}x\mathrm{d}t + o(|\omega_\varepsilon|),$$

and then

$$\widetilde{k} \int_0^T \int_{\omega_\varepsilon} \nabla u \cdot \nabla v_\varepsilon^{(j)}\Phi \mathrm{d}x\mathrm{d}t = \int_0^T \int_\Omega w_t (v_\varepsilon^{(j)} - v^{(j)})\Phi \mathrm{d}x\mathrm{d}t$$
$$+ \widetilde{k} \int_0^T \int_{\omega_\varepsilon} \nabla u^\varepsilon \cdot \nabla v^{(j)}\Phi \mathrm{d}x\mathrm{d}t + \widetilde{k} \int_0^T \int_{\omega_\varepsilon} \nabla u \cdot \nabla\Phi (v^{(j)} - v_\varepsilon^{(j)})\mathrm{d}x\mathrm{d}t + o(|\omega_\varepsilon|)$$
$$= \int_0^T \int_\Omega w_t (v_\varepsilon^{(j)} - v^{(j)})\Phi \mathrm{d}x\mathrm{d}t + \widetilde{k} \int_0^T \int_{\omega_\varepsilon} \nabla u^\varepsilon \cdot \nabla v^{(j)}\Phi \mathrm{d}x\mathrm{d}t + o(|\omega_\varepsilon|). \tag{A.3}$$

Consider the first term in the last line of (A.3). Integrating by parts in time and recalling that $\Phi(T) = 0$, $w(0) = 0$, $(v^{(j)} - v_\varepsilon^{(j)})_t = 0$, we finally have (see also (22) and (47)), for $\varepsilon \to 0$,

$$\int_0^T \int_\Omega w_t(v_\varepsilon^{(j)} - v^{(j)})\Phi \mathrm{d}x\mathrm{d}t = \int_\Omega [w(v_\varepsilon^{(j)} - v^{(j)})\Phi](T)\mathrm{d}x - \int_\Omega [w(v_\varepsilon^{(j)} - v^{(j)})\Phi](0)\mathrm{d}x$$
$$- \int_0^T \int_\Omega \Big(w(v_\varepsilon^{(j)} - v^{(j)})_t\Phi + w(v_\varepsilon^{(j)} - v^{(j)})\Phi_t \Big)\mathrm{d}x\mathrm{d}t = - \int_0^T \int_\Omega w(v_\varepsilon^{(j)} - v^{(j)})\Phi_t \mathrm{d}x\mathrm{d}t = o(|\omega_\varepsilon|). \tag{A.4}$$

Combining (A.3) and (A.4) we get

$$\widetilde{k} \int_0^T \int_{\omega_\varepsilon} \nabla u \cdot \nabla v_\varepsilon^{(j)} \Phi \mathrm{d}x\mathrm{d}t = \widetilde{k} \int_0^T \int_{\omega_\varepsilon} \nabla u^\varepsilon \cdot \nabla v^{(j)} \Phi \mathrm{d}x\mathrm{d}t + o(|\omega_\varepsilon|), \quad \varepsilon \to 0, \tag{A.5}$$

then formula (48) is true.

A.2. Proof of proposition 6.1

Setting $Z(t) = \Phi(T - t)$, $t \in (0, T)$, we get an equivalent problem to (65)

$$\begin{cases} Z_t - k_0 \Delta Z + f'(u)Z = 0, & \text{in } \Omega \times (0, T), \\ \frac{\partial Z}{\partial n} = u^\varepsilon - u, & \text{on } \partial\Omega \times (0, T), \\ Z(0) = 0, & \text{in } \Omega. \end{cases} \tag{A.6}$$

We prove that $Z \in L^2(0, T; H^3(K)) \hookrightarrow L^1(0, T; W^{1,\infty}(K))$. To this aim we derive some energy estimates. Multiplying the first equation in (A.6) by Z, by Young's inequality it holds

$$\frac{1}{2}\frac{\mathrm{d}}{\mathrm{d}t}\|Z(t)\|^2_{L^2(\Omega)} + \frac{k_0}{2}\|\nabla Z(t)\|^2_{L^2(\Omega)} \leqslant C(\|Z(t)\|^2_{L^2(\Omega)} + \|(u^\varepsilon - u)(t)\|^2_{L^2(\partial\Omega)}), \tag{A.7}$$

where $C = C(k_0, M_2, \Omega) > 0$. An application of Gronwall's lemma gives

$$\|Z(t)\|^2_{L^2(\Omega))} \leqslant C\|u^\varepsilon - u\|^2_{L^2(0,t;L^2(\partial\Omega))}, \quad t \in (0, T),$$

so that

$$\|Z\|^2_{L^\infty(0,t;L^2(\Omega))} \leqslant C\|u^\varepsilon - u\|^2_{L^2(0,t;L^2(\partial\Omega))}, \quad t \in (0, T). \tag{A.8}$$

Instead, integrating (A.7) in time over $[0, t]$ we get

$$\int_0^t \|\nabla Z(s)\|^2_{L^2(\Omega)}\mathrm{d}s \leqslant C\left(\int_0^t \|Z(s)\|^2_{L^2(\Omega)}\mathrm{d}s + \int_0^t \|(u^\varepsilon - u)(s)\|^2_{L^2(\partial\Omega)}\mathrm{d}s \right)$$

and finally

$$\|\nabla Z\|^2_{L^2(0,t;L^2(\Omega))} \leqslant C\|u^\varepsilon - u\|^2_{L^2(0,t;L^2(\partial\Omega))}, \quad \forall\, t \in [0, T], \tag{A.9}$$

where C is a positive constant depending on k_0, M_2, Ω, T. We remark that, by standard regularity results, Z is smooth on $E \times [0, T]$, for any compact $E \subset \Omega$.

Consider now two compact sets K_1 and K_2 such that

$$K \subset K_2 \subset K_1 \subset \Omega, \quad d(k_0, \partial\Omega) \geqslant d_1 > 0.$$

It is possible to construct two functions ξ_1, ξ_2 and two constants b_1, b_2 satisfying

$$\xi_i \in C^2(\overline{\Omega}), \quad 0 \leqslant \xi_i \leqslant 1, \quad \xi_i(x) = 1 \quad \forall\, x \in K_i, \quad \xi_i(x) = 0 \quad \forall\, x \in B_i \quad i = 1, 2,$$

$$B_i = \{x \in \Omega \,:\, \mathrm{d}(x, \partial\Omega) \leqslant b_i\}, \quad 0 < b_1 < b_2 < d_1, \quad K \subset\subset \operatorname{Supp} \xi_2 \subset\subset K_1 \subset \operatorname{Supp} \xi_1 \subset \Omega.$$

Let us multiply the first equation of (65) by $-\Delta Z$. Then it holds

$$\frac{\mathrm{d}}{\mathrm{d}t}\left(\frac{1}{2}|\nabla Z|^2\right) + k_0(\Delta Z)^2 - f'(u)Z\Delta Z = \operatorname{div}(Z_t \nabla Z). \tag{A.10}$$

Multiplying (A.10) by ξ_1, integrating on $\Omega \times (0, T)$ and using the definitions of Z, we get

$$\int_\Omega \left(\frac{1}{2}|\nabla Z(T)|^2\right)\xi_1 \mathrm{d}x + k_0 \int_0^T \int_\Omega (\Delta Z)^2 \xi_1 \mathrm{d}x\mathrm{d}t = \int_0^T \int_\Omega f'(u) Z \Delta Z \xi_1 \mathrm{d}x\mathrm{d}t - \int_0^T \int_\Omega Z_t \nabla Z \cdot \nabla \xi_1 \mathrm{d}x\mathrm{d}t. \tag{A.11}$$

Combining (A.11) and the first equation in (A.6), applying Young's inequality and taking into account (25) and the fact that $0 \leqslant \xi \leqslant 1$, we obtain

$$\int_\Omega |\nabla Z(T)|^2 \xi_1 \mathrm{d}x + k_0 \int_0^T \int_\Omega (\Delta Z)^2 \xi_1 \mathrm{d}x\mathrm{d}t \leqslant 2M_2 \int_0^T \int_\Omega Z^2 \mathrm{d}x\mathrm{d}t - 2\int_0^T \int_\Omega (k_0 \Delta Z - f'(u)Z)\nabla Z \cdot \nabla \xi_1 \mathrm{d}x\mathrm{d}t.$$

Integrating by parts the term $\int_0^T \int_\Omega \Delta Z \nabla Z \cdot \nabla \xi_1 \mathrm{d}x\mathrm{d}t$, we easily deduce

$$\int_\Omega |\nabla Z(T)|^2 \xi_1 \mathrm{d}x + \int_0^T \int_\Omega (\Delta Z)^2 \xi_1 \mathrm{d}x\mathrm{d}t \leqslant C\left(\|Z\|^2_{L^2(0,T;L^2(\Omega))} + \|\nabla Z\|^2_{L^2(0,T;L^2(\Omega))}\right), \tag{A.12}$$

where C is a positive constant depending on M_2, k_0, ξ_1. Hence, since $\xi_1 = 1$ in k_0, we get

$$\|\Delta Z\|^2_{L^2(0,T;L^2(K_1))} \leqslant C\left(\|Z\|^2_{L^2(0,T;L^2(\Omega))} + \|\nabla Z\|^2_{L^2(0,T;L^2(\Omega))}\right). \tag{A.13}$$

Observe that, replacing T by $t \in (0, T]$ in (A.12), we deduce also

$$\|\nabla Z\|_{L^\infty(0,T;L^2(K_1))} \leqslant C\left(\|Z\|^2_{L^2(0,T;L^2(\Omega))} + \|\nabla Z\|^2_{L^2(0,T;L^2(\Omega))}\right). \tag{A.14}$$

Combining (A.8), (A.13) and (A.14), we obtain

$$\|Z\|^2_{L^2(0,T;H^2(K_1))} \leqslant C\|u^\varepsilon - u\|^2_{L^2(0,T;L^2(\partial\Omega))}, \tag{A.15}$$

where C is a positive constant depending on $k_0, M_2, \Omega, T, \xi_1$.

On account of the first equation in (A.6) and the previous estimates, we get

$$\|Z_t\|^2_{L^2(0,T;L^2(K_1))} \leqslant C(\|Z\|^2_{L^2(0,T;L^2(\Omega))} + \|\nabla Z\|^2_{L^2(0,T;L^2(\Omega))}) \leqslant C\|u^\varepsilon - u\|^2_{L^2(0,T;L^2(\partial\Omega))}, \tag{A.16}$$

where C is a positive constant depending on $k_0, M_2, \Omega, T, \xi_1$.

Now, let us multiply the first equation of (A.6) by $-\Delta Z_t$. We obtain

$$-Z_t \Delta Z_t + \frac{k_0}{2}\frac{\mathrm{d}}{\mathrm{d}t}(\Delta Z)^2 - f'(u)Z\Delta Z_t = 0.$$

Multiplying the previous equation by ξ_2 and integrating on $\Omega \times (0, T)$, then a suitable integration by parts in space implies

$$\int_0^T \int_\Omega |\nabla Z_t|^2 \xi_2 \mathrm{d}x\mathrm{d}t + \frac{k_0}{2} \int_0^T \int_\Omega \frac{\mathrm{d}}{\mathrm{d}t} (\Delta Z)^2 \xi_2 \mathrm{d}x\mathrm{d}t$$

$$+ \int_0^T \int_\Omega \xi_2 Z f''(u) \nabla u \cdot \nabla Z_t \mathrm{d}x\mathrm{d}t + \int_0^T \int_\Omega \xi_2 f'(u) \nabla Z \cdot \nabla Z_t \mathrm{d}x\mathrm{d}t$$

$$= \int_0^T \int_\Omega \mathrm{div} \left(\frac{1}{2} \nabla ((Z_t)^2) \right) \xi_2 \mathrm{d}x\mathrm{d}t + \int_0^T \int_\Omega \mathrm{div} \left(\nabla (f'(u) Z Z_t) \mathrm{d}x\mathrm{d}t - Z_t \nabla (f'(u) Z) \right) \xi_2 \mathrm{d}x\mathrm{d}t.$$

Integrating by parts in time the second term of the left-hand side and by parts in space the terms in the right-hand side, by an application of Young's inequality we finally get

$$\int_0^T \int_{K_2} |\nabla Z_t|^2 \mathrm{d}x\mathrm{d}t \leqslant \int_0^T \int_\Omega |\nabla Z_t|^2 \xi_2 \mathrm{d}x\mathrm{d}t \leqslant C \left(\int_0^T \int_\Omega |Z|^2 \mathrm{d}x\mathrm{d}t + \int_0^T \int_\Omega |\nabla Z|^2 \mathrm{d}x\mathrm{d}t + \int_0^T \int_{K_1} (Z_t)^2 \mathrm{d}x\mathrm{d}t \right),$$

where the constant $C > 0$ depends on ξ_2, M_2. A combination with (A.8), (A.9) and (A.16) gives

$$\|\nabla Z_t\|^2_{L^2(0,T;L^2(K_2))} \leqslant C \|u^\varepsilon - u\|^2_{L^2(0,T;L^2(\partial\Omega))},$$

where the constant $C > 0$ depends on $k_0, M_2, \Omega, T, \xi_1, \xi_2$. In order to prove the desired regularity, we need to take into account also the third-order derivatives, in particular the operator $\nabla \Delta Z$. Observe that from the first equation in (A.6) we get

$$\nabla \Delta Z = \frac{1}{k_0} \left(\nabla Z_t + Z f''(u) \nabla u + f'(u) \nabla Z \right). \tag{A.17}$$

Hence, we can conclude

$$\|\nabla \Delta Z\|^2_{L^2(0,T;L^2(K_2))} \leqslant C \|u^\varepsilon - u\|^2_{L^2(0,T;L^2(\partial\Omega))},$$

where C is a positive constant depending on $k_0, \frac{1}{k_0}, M_2, \Omega, T, \xi_1, \xi_2$.

Recalling (A.15) and the fact that $K \subset K_2 \subset K_1$, standard regularity results imply

$$\|Z\|^2_{L^2(0,T;H^3(K))} \leqslant C \|u^\varepsilon - u\|^2_{L^2(0,T;L^2(\partial\Omega))}. \tag{A.18}$$

Finally, from (A.15) and (A.18), by Sobolev immersion theorems, we get

$$\|Z\|^2_{L^1(0,T;W^{1,\infty}(K))} \leqslant C(T) \|Z\|^2_{L^2(0,T;W^{1,\infty}(K))} \leqslant C \|u^\varepsilon - u\|^2_{L^2(0,T;L^2(\partial\Omega))}, \tag{A.19}$$

where C is a positive constant depending on $k_0, \frac{1}{k_0}, M_2, \Omega, T, \xi_1, \xi_2$.

Recalling the relation between Z and Φ we get (66).

ORCID iDs

Cecilia Cavaterra https://orcid.org/0000-0002-2754-7714
Andrea Manzoni https://orcid.org/0000-0001-8277-2802
Luca Ratti https://orcid.org/0000-0001-7948-0577

References

[1] Álvarez D, Alonso-Atienza F, Rojo-Álvarez J L, Garcia-Alberola A and Moscoso M 2012 Shape reconstruction of cardiac ischemia from non-contact intracardiac recordings: a model study *Math. Comput. Model.* **55** 1770–81

[2] Ammari H, Garapon P, Jouve F, Kang H, Lim M and Yu S 2013 A new optimal control approach for the reconstruction of extended inclusions *SIAM J. Control Optim.* **51** 1372–94

[3] Ammari H, Garnier J, Jugnon V and Kang H 2012 Stability and resolution analysis for a topological derivative based imaging functional *SIAM J. Control Optim.* **50** 48–76

[4] Ammari H, Iakovleva E, Kang H and Kim K 2005 Direct algorithms for thermal imaging of small inclusions *Multiscale Model. Simul.* **4** 1116–36

[5] Ammari H and Kang H 2004 *Reconstruction of Small Inhomogeneities from Boundary Measurements* (*Lectures Notes in Mathematics Series* vol 1846) (Berlin: Springer)

[6] Aras K, Burton B, Swenson D and MacLeod R 2016 Spatial organization of acute myocardial ischemia *J. Electrocardiol.* **49** 323–36

[7] Bendahmane M and Karlsen K H 2006 Analysis of a class of degenerate reaction-diffusion systems and the bidomain model of cardiac tissue *Netw. Heterog. Media* **1** 185–218

[8] Beretta E and Cavaterra C 2011 Identifying a space dependent coefficient in a reaction-diffusion equation *Inverse Probl. Imaging* **5** 285–96

[9] Beretta E, Cerutti M C, Manzoni A and Pierotti D 2016 An asymptotic formula for boundary potential perturbations in a semilinear elliptic equation related to cardiac electrophysiology *Math. Models Methods Appl. Sci.* **26** 645–70

[10] Beretta E, Manzoni A and Ratti L 2017 A reconstruction algorithm based on topological gradient for an inverse problem related to a semilinear elliptic boundary value problem *Inverse Problems* **33** 035010

[11] Boulakia M, Fernández M A, Gerbeau J F and Zemzemi N 2008 A coupled system of PDEs and ODEs arising in electrocardiograms modeling *Appl. Math. Res. Exp.* **2008**

[12] Boulakia M, Schenone E and Gerbeau J-F 2012 Reduced-order modeling for cardiac electrophysiology application to parameter identification *Int. J. Numer. Meth. Biomed. Eng.* **28** 727–44

[13] Bourgault Y, Coudière Y and Pierre C 2009 Existence and uniqueness of the solution for the bidomain model used in cardiac electrophysiology *Nonlinear Anal. Real World Appl.* **10** 458–82

[14] Burger M, Mardal K A and Nielsen B F 2010 Stability analysis of the inverse transmembrane potential problem in electrocardiography *Inverse Problems* **26** 105012

[15] Capdeboscq Y and Vogelius M 2003 A general representation formula for boundary voltage perturbations caused by internal conductivity inhomogeneities of low order fraction *ESAIM: Math. Model. Numer. Anal.* **37** 159–73

[16] Cedio-Fengya D J, Moskow S and Vogelius M 1998 Identification of conductivity imperfections of small diameter by boundary measurements continuous dependence and computational reconstruction *Inverse Problems* **14** 553–95

[17] Chaabane S, Masmoudi M and Meftahi H 2013 Topological and shape gradient strategy for solving geometrical inverse problems *J. Math. Anal. Appl.* **400** 724–42

[18] Chávez C E, Zemzemi N, Coudière Y, Alonso-Atienza F and Álvarez D 2015 Inverse problem of electrocardiography: estimating the location of cardiac ischemia in a 3D realistic geometry *Proc. 8th Int. Conf. Functional Imaging and Modeling of the Heart (Maastricht, The Netherlands, 25–27 June 2015)* ed H van Assen *et al* (Berlin: Springer)

[19] Franzone P C, Pavarino L and Scacchi S 2007 Dynamical effects of myocardial ischemia in anisotropic cardiac models in three dimensions *Math. Models Methods Appl. Sci.* **17** 1965–2008

[20] Franzone P C, Pavarino L and Scacchi S 2014 *Mathematical Cardiac Electrophysiology* (*Modeling, Simulation and Applications Series* vol 13) (New York: Springer)

[21] Franzone P C, Taccardi B and Viganotti C 1978 An approach to inverse calculation of epicardial potentials from body surface maps *Adv. Cardiol.* **21** 50–4

[22] Di Cristo M and Vessella S 2010 Stable determination of the discontinuous conductivity coefficient of a parabolic equation *SIAM J. Math. Anal.* **42** 183–217

[23] Dung L 2000 Remarks on Hölder continuity for parabolic equations and convergence to global attractors *Nonlinear Anal.* **41** 921–41

[24] Elayyan A and Isakov V 1997 On uniqueness of recovery of the discontinuous conductivity coefficient of a parabolic equation *SIAM J. Math. Anal.* **28** 49–59

[25] Fernández M and Zemzemi N 2010 Decoupled time-marching schemes in computational cardiac electrophysiology and ECG numerical simulation *Math. Biosci.* **226** 58–75
[26] Friedman A and Vogelius M 1984 Identification of small inhomogeneities of extreme conductivity by boundary measurements: a theorem on continuous dependence *Arch. Ration. Mech. Anal.* **105** 299–326
[27] Gerbeau J F, Lombardi D and Schenone E 2015 Reduced order model in cardiac electrophysiology with approximated Lax pairs *Adv. Comput. Math.* **41** 1103–30
[28] Gilbarg D and Trudinger N S 1983 *Elliptic Partial Differential Equations of Second Order* (Berlin: Springer)
[29] He Y and Keyes D E 2013 Large-scale parameter extraction in electrocardiology models through Born approximation *Inverse Problems* **29** 015001
[30] Isakov V 1993 On uniqueness in inverse problems for semilinear parabolic equations *Arch. Ration. Mech. Anal.* **124** 1–12
[31] Isakov V 2017 *Inverse Problems for Partial Differential Equations* 3rd edn (*Applied Mathematical Sciences Series* vol 127) (Berlin: Springer)
[32] Isakov V, Kim K and Nakamura G 2010 Reconstruction of an unknown inclusion by thermography *Ann. Scuol. Norm. Super. Pisa-Classe Sci.* **9** 725–58
[33] Ladyzenskaja O A, Solonnikov V A and Ural'ceva N N 1968 *Linear and Quasi-linear Equations of Parabolic Type* (*AMS Translations Monographs* vol 23) (Providence, RI: American Mathematical Society)
[34] Lunardi A 1995 *Analytic Semigroups and Optimal Regularity in Parabolic Problems* (Basel: Birkhäuser)
[35] Lysaker M and Nielsen B F 2006 Towards a level set framework for infarction modeling: an inverse problem *Int. J. Numer. Anal. Model.* **3** 377–94
[36] Nakamura G and Sasayama S 2013 Inverse boundary value problem for the heat equation with discontinuous coefficients *J. Inverse lll-Posed Probl.* **21** 217–32
[37] Nielsen B F, Lykaser M and Tveito A 2007 On the use of the resting potential and level set methods for identifying ischemic heart disease: an inverse problem *J. Comput. Phys.* **220** 772–90
[38] Nirenberg L 1959 On elliptic partial differential equations *Ann. Scuola Norm. Super. Pisa* **13** 115–62
[39] Pao C V 1992 *Nonlinear Parabolic and Elliptic Equations* (New York: Plenum)
[40] Park W K 2012 Topological derivative strategy for one-step iteration imaging of arbitrary shaped thin, curve-like electromagnetic inclusions *J. Comput. Phys.* **231** 1426–39
[41] Pullan A J, Cheng L K, Nash M P, Ghodrati A, MacLeod R and Brooks D H 2010 The inverse problem of electrocardiography *Comprehensive Electrocardiology* ed P W Macfarlane *et al* (London: Springer) pp 299–344
[42] Quarteroni A, Lassila T, Rossi S and Ruiz-Baier R 2017 Integrated heart—coupling multiscale and multiphysics models for the simulation of the cardiac function *Comput. Methods Appl. Mech. Eng.* **314** 345–407
[43] Robinson J C 2001 *Infinite-Dimensional Dynamical Systems* (*Cambridge Texts in Applied Mathematics*) (Cambridge: Cambridge University Press)
[44] Rossi S, Lassila T, Ruiz-Baier R, Sequeira A and Quarteroni A 2014 Thermodynamically consistent orthotropic activation model capturing ventricular systolic wall thickening in cardiac electromechanics *Eur. J. Mech.* A **48** 129–42
[45] Ruud T S, Nielsen B F, Lysaker M and Sundnes J 2009 A computationally efficient method for determining the size and location of myocardial ischemia *IEEE Trans. Biomed. Eng.* **56** 263–72
[46] Sanfelici S 2002 Convergence of the Galerkin approximation of a degenerate evolution problem in electrocardiology *Numer. Methods PDE* **18** 218–40
[47] Sundnes J, Lines G T, Cai X, Nielsen B F, Mardal K A and Tveito A 2006 *Computing the Electrical Activity in the Heart* (*Monographs in Computational Science and Engineering Series* vol 1) (Berlin: Springer)
[48] Negri F 2016 redbKIT Version 2.2 (http://redbkit.github.io/redbKIT)